View metadata, citation and similar papers at core.ac.uk

brought to you by CORE

provided by Digital.CSIC

Elsevier Editorial System(tm) for Journal of Volcanology and Geothermal Research
Manuscript Draft

Manuscript Number: VOLGEO3647R1

Title: Cyclic growth and mass wasting of submarine Los Frailes lava flow and dome complex in Cabo de Gata, SE Spain

Article Type: Research Paper

Keywords: Sector collapse; Debris avalanche; Submarine domes; Pumice flow

Corresponding Author: Dr Carles Soriano,

Corresponding Author's Institution: Institut Jaume Almera, CSIC

First Author: Carles Soriano

Order of Authors: Carles Soriano; Nancy Riggs; Guido Giordano; Massimiliano Porreca; Sandro Conticelli

Abstract: The Los Frailes Formation lava-flow and dome complex is a Miocene succession that is part of the Cabo de Gata volcanic zone of SE Spain. The complex comprises dominantly dacitic, subaqueous dome rocks and interstratified sedimentary horizons emplaced over a few tens of thousands of years. Facies of the Los Frailes Formation include coherent lava, in-situ hyaloclastite, locally with microfossil-bearing siltstone matrix, pumiceous and block-rich tuff, and massive monomict breccia and megabreccia, in which clasts are locally several meters in diameter. The monomict megabreccias display both "block facies" and "matrix facies" architecture and show internal deformation at the block-matrix contacts. They are inferred to have derived from debris avalanches. Facies are divided into four volcanic units separated by fossiliferous marine sedimentary units emplaced during hiatuses in volcanism.
The Los Frailes Formation lava-flow and dome complex was emplaced in a shallow setting that may have included emergent areas. Lava flows and the margins of dome edifices interacted with sea water to form hyaloclastite, and pyroclastic currents deposited pumiceous materials. Sector collapse of marine domes fed small-volume debris avalanches with generally the same facies and distribution of facies as the larger-scale equivalents on which traditional models are built.

Revision Notes
Click here to download Revision Notes: Revised VOLGEO3647.doc

Dear Prof.Wilson,

We are sending the revised version of ms "Cyclic growth and mass wasting of submarine Los Frailes lava flow and dome complex in Cabo de Gata, SE Spain" by Soriano et al. for submission to JVGR. We appreciate reviews by A. Belousov and J-L. Schneider, which have notably improved the ms.
Most of the comments made by both reviewers in their annotated copies have been directly addressed in this new version, which has been checked for grammar and style by the English-speaking author. As a result many sentences have been partly rewritten accordingly to the reviewers' suggestions. Below we address the main reviewer's comments.
Table 2 has been improved by adding rock type, geographic coordinates and stratigraphic position of samples.
A new table, Table 3, has been added to the ms with the diagnostic features of lithofacies and their interpretation.
The chronostratigraphic relation of dikes with the defined stratigraphic units has been constrained more precisely in sections 3.2 and 7.2.
References and citations have been checked.
Thickness of debris avalanche deposits has been discussed in section 7.1.
Fig. 2 has been ameliorated as suggested by both reviewers.
Lava flow and dome lithofacies, in particular hyaloclastite breccia facies, have been partly rewritten throughout the text and their facies architecture has been characterized in order to obtain a more comprehensive facies model. Consequently, Figs. 4 and 5 have changed its order and former Fig. 4a has been substituted by photographs illustrating the subaqueous emplacement of magma. However, we would like to emphasize that jigsaw fit texture (coupled with lithofacies gradation) is indeed characteristic of quench fragmentation and emplacement of magma in subaqueous conditions. It was first described in the early papers on hyaloclastite (i.e. Pichler, 1965) and later on debris avalanche deposits, in particular after the Mt. St. Helens event.
The submarine emplacement of volcanic rocks has been better constrained with a more comprehensive facies model of magma emplacement in subaqueous conditions and also by emphasizing that lavas and volcaniclastic are interbedded with sediments containing unambiguous marine fossils. However, it is beyond the scope of this ms to undertake a paleoenvironment investigation, which would require a detailed study of fossils at the species level.
Finally, we agree with comment by J-L. Schneider on Fig. 12. The beach conglomerate on top of the lavas can be much younger than magma emplacement and therefore it cannot be interpreted as evidence of an emergent lava dome. Consequently, Fig. 12 and the section in the text devoted to this figure have been omitted.

We hope that now this ms is suitable for publication in JVGR and again comments by both reviewers are much appreciated.

Yours sincerely,

Carles

***Highlights**

Volcanism is cyclic and interrupted by periods of carbonate and siliciclastic deposition. > Volcanic cycles consist of effusive and explosive events and volcano mass wasting. > Sector collapse of Miocene submarine lava flows and domes yielded debris avalanche deposits.

*Manuscript
Click here to view linked References

Cyclic growth and mass wasting of submarine Los Frailes lava flow and dome complex in Cabo de Gata, SE Spain

Carles Soriano[a,*], Nancy Riggs[b], Guido Giordano[c], Massimiliano Porreca[d], Sandro Conticelli[e,f]

[a] Institut de Ciències de la Terra Jaume Almera, CSIC, c/ Lluís Solé Sabarís s/n, Barcelona 08028, Spain, Tel. +34934095410, Fax +34934110012, E-mail address: csoriano@ija.csic.es

[b] Department of Geology, Northern Arizona University, Flagstaff AZ 86011, USA, E-mail:
nancy.riggs@nau.edu

[c] Dipartimento di Scienze Geologiche, Università degli Studi Roma Tre, Largo S. Leonardo Murialdo 1, 00146, Roma, Italy, E-mail: giordano@uniroma3.it

[d] Centro de Vulcanologia e Avaliação de Riscos Geológicos (CVARG), Departamento de Geociências, Universidade dos Açores, Complexo Científico, 2º Piso, 9500-801 Ponta Delgada, Portugal, E-mail: Massimiliano.Porreca@azores.gov.pt

[e] Dipartimento di Scienze della Terra, Università degli Studi di Firenze, Via G. La Pira, 4, I-50121, Firenze, Italy, E-mail: sandro.conticelli@unifi.it

[f] Sezione di Firenze of the Istituto di Geoscienze e Georisorse, Consiglio Nazionale delle Ricerche, Via G. La Pira, 4, I-50121, Firenze, Italy

*Corresponding author

Abstract

The Los Frailes Formation lava-flow and dome complex is a Miocene succession that is part of the Cabo de Gata volcanic zone of SE Spain. The complex comprises dominantly dacitic, subaqueous dome rocks and interstratified sedimentary horizons emplaced over a few tens of thousands of years. Facies of the Los Frailes Formation include coherent lava, in-situ hyaloclastite, locally with microfossil-bearing siltstone matrix, pumiceous and block-rich tuff, and massive monomict breccia and megabreccia, in which clasts are locally several meters in diameter. The monomict megabreccias display both “block facies” and “matrix facies” architecture and show internal deformation at the block-matrix contacts. They are inferred to have derived from debris avalanches. Facies are divided into four volcanic units separated by fossiliferous marine sedimentary units emplaced during hiatuses in volcanism.

The Los Frailes Formation lava-flow and dome complex was emplaced in a shallow setting that may have included emergent areas. Lava flows and the margins of dome edifices interacted with sea water to form hyaloclastite, and pyroclastic currents deposited pumiceous materials. Sector collapse of marine domes fed small-volume debris avalanches with generally the same facies and distribution of facies as the larger-scale equivalents on which traditional models are built.

Keywords: Sector collapse; Debris avalanche; Submarine domes; Pumice flow

1. Introduction

Understanding submarine volcanic processes and reconstructing submarine volcanic edifices and their associated processes have been primarily based on the study of ancient volcanic successions (Fiske and Matsuda, 1964; Cas et al., 1990; McPhie et

al., 1993; Kano et al., 1996; De Rita et al., 2001; White et al., 2003 and references therein). However, in the last decade an increasing number of submarine surveys undertaken in active volcanic systems (e.g. the ongoing NOOA Vents Program http://www.pmel.noaa.gov/vents/marianas_site.html) have notably improved the knowledge of submarine volcanism and of the architecture of submarine volcanoes (Fiske et al. 2001; Wright, 2001; Trofimovs et al., 2006; Chadwick et al., 2008; Walker et al., 2008; Leat et al., 2010). Nevertheless, research on modern submarine volcanoes is relatively recent and rather expensive when compared to research on ancient submarine successions. For these reasons, very few of submarine surveys on modern volcanoes are able to document volcano evolution through eruptive and non-eruptive periods (Chadwick et al., 2008).

The Miocene Los Frailes Formation in Cabo de Gata, SE Spain (Fig. 1), is a volcanic unit dominated by volcaniclastic deposits and also includes carbonate and siliclastic deposits sedimented during periods of volcanic quiescence. This study includes facies analysis, $^{40}Ar/^{39}Ar$ dating and characterization of the petrography and geochemistry to propose a facies and volcanic evolution model for the Los Frailes Formation. The results are compared to the volcano dynamics of modern analogues, aiming to contribute a better understanding of the evolution of a multi-cyclic submarine volcanic system over a time period tens of thousands of years long.

2. Geologic setting

The Alborán Domain is a northeast-trending volcanic zone that extends from the North African coast to the southeastern coast of Spain. This area is up to 200 km wide and 400 km long and comprises volcanic rocks of the southeastern coast of the Iberian

Peninsula (i.e., Malaga, Cabo de Gata, Mazarrón, and Murcia), the North African coast between Nador in Morocco and Oran in Algeria, and the Alborán Island and surrounding seamounts, together with Neogene intramontane sedimentary basins. The Alborán Domain is located in the internal part of the Betic-Rif orogenic belt, which is composed of Paleozoic and Triassic metamorphic rocks of the Alpujárride and Nevado-Filábride complexes. Volcanism is roughly coeval with extension, rifting, and seafloor spreading in the Alborán basin and with the collision between the African and European plates, which constitutes a long-standing paradox (Dewey et al., 1989). Several often contradictory tectonomagmatic models have been proposed for this region, partly trying to explain this paradox (see Doblas et al. 2007 for details).

Volcanism accompanied and post-dated Neogene extension in the Alborán and Rif basins. Volcanism is characterized by arc-tholeiitic, calc-alkaline, shoshonitic and ultrapotassic (lamproitelike) rocks (e.g., Venturelli et al., 1984; Torres-Roldán et al., 1986; Benito et al., 1999; Turner et al., 1999; Duggen et al., 2005; Prelević et al., 2008; Conticelli et al., 2009; Tommasini et al., 2011) all with orogenic signatures, but within-plate alkalibasalts occur during the last stages of the basin evolution (e.g., Duggen et al. 2005). The calc-alkaline rocks are volumetrically predominant, are concentrated in the central part of the domain (Alborán Island and surrounding seamounts, and Cabo de Gata volcanic zone), and are older than ultra-potassic volcanic rocks. Within-plate alkali-basalts occur predominantly in the northern and southern sectors of the Alborán domain and are separated from the calc-alkaline igneous rocks by a hiatus of some million years (Duggen et al., 2005).

The Neogene Cabo de Gata volcanic zone forms part of the Almeria-Níjar basin (Fig. 1), which is one of the intramontane volcano-sedimentary basins of the Alborán Domain, within the internal areas of the Betic-Rif orogen (Montenat and Ott d'Estevou,

1990; Sáenz de Galdeano and Vera, 1992). It is bounded to the NW by the Carboneras fault zone, a sinistral strike-slip structure active since late Oligocene to present days (Scotney et al., 2000; Reicherter and Hübscher, 2007), and to the SE by the coastline (Fig. 1). Sedimentary rocks of the Cabo de Gata volcanic zone are dominantly temperate-carbonate deposits but also include siliciclastic sediments (Fernández Soler, 1987; Di Battistini et al., 1987; Serrano, 1992; Martín et al., 1996). Volcanic rocks range from calc-alkaline to high-K calc-alkaline and shoshonitic, with rock terms from basaltic andesite to high-K rhyolite and trachyte (Benito et al., 1999; Turner et al., 1999; Duggen et al., 2005; Conticelli et al., 2009). Paleozoic and Triassic metamorphic rocks of the Alpujárride and Nevado-Filábride complexes are the basement to the Neogene succession, and are exposed in areas adjacent to the Cabo de Gata volcanic zone and along the Carboneras fault zone. Volcanism is effusive and explosive exhibiting a wide variety of volcanic and volcaniclastic facies. The original morphologies of volcanic edifices are poorly preserved due to erosion, although good sections of deposits crop out on marine cliffs and inland exposures.

3. Volcanic succession of the Los Frailes area

The Los Frailes area is located in the southwest of the Cabo de Gata volcanic zone and is dominated by Cerro de Los Frailes, a hill that rises to 493 meters a.s.l. (*above sea level*) with gentle slopes that yield to 30-meter-high marine cliffs on the coastline (Figs. 1 and 2). Rocks forming Cerro de Los Frailes and adjacent areas are in contact to the northeast with rocks of the younger Rodalquilar Group and to the southwest with high-K volcanic rocks of the southwestern Cabo de Gata volcanic zone (Fuster et al., 1965; Cunnhingham et al., 1990; Arribas, 1993; Fernández-Soler, 2001).

The Los Frailes area has been mapped at 1:10000, providing a general stratigraphy of the area. Stratigraphic logs in Figure 3 are composite sections. The stratigraphic succession of Los Frailes area is characterized by thick intervals of volcanic and volcaniclastic rocks interbedded with thinner layers of sedimentary rocks. Volcanic rocks range from basaltic andesite to dacite and rhyolite, while sedimentary rocks are mostly carbonate but also include conglomerate, sandstone, and siltstone (Fuster et al., 1965; Di Battistini et al., 1987; Fernandez Soler, 1987; Cunningham et al., 1990). Planktonic foraminifera assemblages in Los Frailes and adjacent areas are assigned to the Serravallian and Tortonian stages of the Miocene (Serrano, 1992).

The volcano-sedimentary succession of Los Frailes area is here divided into lithostratigraphic units based on lithology, composition, and stratigraphic position. We have chosen to define new formal units by following the guidelines of the International Commission on Stratigraphy (http://www.stratigraphy.org/) instead of using informal units previously defined. The equivalence of these units to other chronostratigraphic schemes proposed for this area and their estimated position in the geological time scale is shown in Table 1.

3.1 Caliguera Formation

The Caliguera Formation is mostly composed of massive monomict andesite breccia occasionally interbedded with monomict andesitic sandstone. This unit is mainly exposed in the Cala de la Higuera beach and farther to the northwest where it also consists of coherent andesite lava (Fig. 2). Andesite of the Caliguera Formation is dark grey to dark green and porphyritic, with plagioclase and pyroxene phenocrysts embedded in a groundmass of plagioclase microlites partly altered to chlorite. Massive

breccia is poorly sorted and matrix to clast supported with angular to subangular, centimetre to decimetre clasts. The lower contact of this unit is not exposed while the uppermost andesite underlies beds of the Los Frailes Formation along an irregular contact. Maximum thickness in outcrop of the Caliguera Formation is about 50 meters.

3.2 Los Frailes Formation

The Los Frailes Formation is named for exposures on the lower slopes of Cerro de Los Frailes, but extends farther to the north, west and southwest (Fig. 2). It is mainly composed of dacite breccia, lava and pyroclastic rocks that are pale brown to pale grey and amphibole to biotite rich. The upper part of this unit is characterized by a sedimentary interval up to 50 m thick that comprises conglomerate, sandstone, and bioclastic carbonate (Figs. 2 and 3). Around Cerro de Los Frailes, the Los Frailes Formation is overlain by rocks of the Cerro La Palma Formation whereas farther to the north it is overlain by rhyodacite lava and breccia and rhyolite tuff of the Rodalquilar Group (Fernández-Soler, 2001). Maximum thickness in outcrop of the Los Frailes Formation is more than 300 meters.

The stratigraphic succession of the Los Frailes Formation comprises thick intervals of volcanic and volcaniclastic rocks interbedded with thinner intervals of sedimentary strata (Fig. 3). This volcano-sedimentary succession has been divided into volcanic or sedimentary units according to their lithology, stratigraphic position and internal discontinuities. In the stratigraphic logs of Figure 3 only volcanic units have been identified for simplicity (Units 1 to 4). Sedimentary units are laterally discontinuous, which results locally in the amalgamation of volcanic units (Figs. 2 and 3). Volcanic units consist of lava and volcaniclastic deposits and are laterally continuous for hundreds of meters to kilometres. Volcanic units and sedimentary units

have been correlated throughout the studied area based on mapping and characteristics of measured stratigraphic logs, and their contacts are discordant and erosionals.

Sedimentary units are dominated by bioclastic carbonate but also include polymict siltstone, sandstone, and conglomerate with phyllite pebbles from the metamorphic basement of the Cabo de Gata volcanic zone. Fossil content include oysters, corals, *Globigerinid* planktonic foraminifera, bryozoans, algae, echinoderms, and undifferentiated shell and wood fragments. Sedimentary structures comprise erosive bases, massive beds, dune cross-bedding and ripple cross-lamination. The dominance of coastal and shallow-marine bioclasts and the sedimentary structures are in agreement with transport and deposition in a shallow-water carbonate environment. This may have included resedimentation of carbonate beach, barrier, and platform deposits and is characteristic in other carbonate sequences of Tortonian age in the Sierra de Gata area (Martín et al., 1996; Johnson et al., 2005). These sediments were deposited during periods of volcanic repose.

Northwest- to northeast trending, subvertical, dominantly dacitic dikes intrude the Los Frailes Formation (Figs. 2 and 3b). These dikes are as much as 100 meters thick and consist of coherent dacite with subvertical flow foliation and subhorizontal columnar jointing. Dacite is porphyritic consisting of phenocrysts of plagioclase and amphibole embedded in a glassy groundmass that contains microlites of plagioclase, clinopyroxene, and k-feldspar. Similar phenocryst assemblage and geochemistry between dikes and volcanic rocks of Los Frailes Formation suggests that they are genetically related (Fig. 4).

3.3. Casa del Tomate Formation

The Casa del Tomate Formation is a massive to cross-bedded and pumice-rich

rhyolite tuff that contains minor clasts of porphyritic dark green andesite from the underlying Caliguera Formation and phyllite clasts derived from the basement of the Cabo de Gata volcanic zone. Matrix is composed of glass shards, broken crystals of quartz and feldspar, and is partly recrystallized along preferred bands to a mosaic of quartz and feldspar crystals. Pumice clasts are subrounded and consist of quartz, feldspar, and biotite phenocrysts in a glassy and vesicular groundmass. The Casa del Tomate Formation crops out in Cala de la Higuera close to a major NW-trending normal fault zone, and farther to the northeast in Casa del Tomate (Fig. 2). At Cala de la Higuera rhyolite tuffs are sheared, showing shear-cleavage structures, veins with secondary quartz, and subvertical bedding planes. The stratigraphic relation of this tuff with other units in the Los Frailes area is unclear, as contacts are poorly exposed and sheared. At Casa del Tomate, the tuff is intruded by subvertical dacite dikes of the Los Frailes Formation.

3.4 Cerro de la Palma Formation

The Cerro la Palma Formation consists of dark grey to black basaltic andesite breccia and coherent lava that cap the prominent Cerro de Los Frailes (Fig. 2). Lavas are columnar jointed and porphyritic with plagioclase, clinopyroxene, and minor olivine phenocrysts embedded in a partly devitrified groundmass of plagioclase microlites. Breccias are monomict, matrix to clast supported and locally show jigsaw-fit of subequant clasts. The top of the Cerro de la Palma Formation is eroded and the maximum preserved thickness is about 300 meters. The base overlies an irregular and erosional surface that truncates beds of the sedimentary interval at the top of dacite breccia and lava of the underlying Los Frailes Formation.

4. Petrography, geochemistry and radio-isotopic dating

The volcanic rocks are typical two-pyroxene calc-alkaline rocks ranging in composition from basaltic andesite to rhyolite, with dacite being the most common rock type (Fig. 4). Forsteritic olivine is restricted to basaltic andesite of the Cerro la Palma Fm. Plagioclase, clinopyroxene and opaque minerals are ubiquitous in all rocks while orthopyroxene is found in andesite of the Caliguera Fm and dacite of the Los Frailes Formation. Biotite is restricted to dacite (Los Frailes Formation) and rhyolite (Casa del Tomate Formation). Rare sanidine is found in rhyolite of the Casa del Tomate Fm and accessory apatite and zircon in the most silicic terms. Supplementary file #1 reports major and trace elements of selected samples from the three formations in the Los Frailes area. These rocks display the lowest alkali content, in particular K2O, among the rocks of the Cabo de Gata volcanic zone (Conticelli et al. 2009). Silica ranges from 54.5 to 71.6 wt.%, with a silica gap between 58 and 62 wt.% (Fig. 4). Other major elements vary linearly with silica in Harker variation diagrams, with positive correlation for alkalis, negative for aluminum, calcium, magnesium, and total iron, and composite correlations for titanium and phosphorous. Trace elements display complex arrays with increasing silica. Sc, V, and Ni behave massively as compatible elements being fractionated by crystallizing phases (Supplementary file #2). Sr aligns along two different paths: the Cerro la Palma samples along a path at lower Sr and Los Frailes samples along a path at higher Sr. Although their incompatible behaviour, Nb, Zr, and Ba display complex arrays, with a drop in Zr and an abrupt change in the Ba in rhyolite samples of the Casa del Tomate Unit (Supplementary file #2).

Two samples from megablocks within volcanic breccia of Units 2 and 4 of the Los Frailes Formation and one sample from coherent lava at the base of the Cerro la Palma Formation (Cerro La Palma stratigraphic log, Fig. 3a) were dated by $^{40}Ar/^{39}Ar$.

An additional sample from the rhyolite tuff of the Casa del Tomate Formation was collected to the northeast of this area. Samples were crushed and prepared for laser incremental heating at the Rare Gas Geochronology Laboratory of the Wisconsin University-Madison. A summary of results with weighted mean ages and isochron ages is provided in Table 2. The obtained ages are stratigraphically consistent, while are slightly older than K-Ar ages by di Battistini et al. (1987). A significant hiatus (~3 m.y.) in the volcanic activity is observed between the Los Frailes Formation and the Cerrro la Palma Formation, with the exception of the rhyolite extrusion of Casa del Tomate at 12.13 Ma.

5. Lithofacies of the Los Frailes Formation

The Los Frailes Formation is composed of lava and volcaniclastic deposits, including different types of volcanic breccia and tuffs. Sedimentary units are present, but a detailed analysis of their lithofacies is beyond the scope of this contribution. Only aspects such as fossil content or contact relations that help characterize the volcanism of the Los Frailes Formation, in particular the environment of volcanic emplacement, are discussed. The main characteristics of volcanic lithofacies of Los Frailes Formation are summarized in Table 3.

5.1. Coherent lava

Coherent lava is porphyritic to glomeroporphyritic, consisting of euhedral plagioclase (~9%), amphibole (~6%), biotite (~3%), and pyroxene (~2%) phenocrysts and opaque minerals set in a microcrystalline groundmass of plagioclase, amphibole, and biotite. Glomeroporphyric aggregates are either monomineralic plagioclase or polymineralic with plagioclase, amphibole and pyroxene. The groundmass locally

shows amygdules and spherulites. Coherent lava is as much as 40 metres thick, displays flow banding with decimetre-scale flow folds and columnar joints, and grades into hyaloclastite breccia (Fig. 5A, B, C).

5.1.1. Interpretation

Porphyritic texture with euhedral phenocrysts and glomeroporphyric aggregates, flow banding, flow folds and columnar jointing indicate emplacement of viscous lava and cooling from above the glass transition temperature. Spherulite is representative of devitrification of volcanic glass.

5.2. Hyaloclastite breccia

Hyaloclastite breccia is a massive monomict breccia exhibiting clast- to matrix-supported domains with gradational contacts. Clasts are porphyritc, subequant and subangular with curviplanar edges, range in size from 1 centimetre to 1 metre and are petrographically identical to coherent lava. They are flow banded and display jigsaw-fit texture with domains in which clasts are slightly rotated (Fig. 5 B). Flow banding can be traced across adjacent clasts in the jigsaw fit texture (Fig. 5C). Matrix is dominantly composed of < 1 centimetre dacite clasts locally with jigsaw fit. Occasionally, the matrix consists of laminated siltstone in which the subhorizontal lamination can be consistently traced between clasts. This siltstone locally contains *Globigerinid* planktonic foraminifera, echinoderm plates and spines, and bryozoa and disappears downward while hyaloclastite breccia grades into coherent lava. This facies is up to 40 metres thick and grades laterally, upward and downward into coherent lava.

5.2.1. Interpretation

Jigsaw-fit of subequant clasts with curviplanar edges is characteristic of quench fragmentation of hot magma in subaqueous conditions (Pichler, 1965; Yamagishi and Dimroth, 1985). Matrix domains with small-size clasts showing jigsaw fit texture is characteristic of thermal granulation of hot magma in subaqueous conditions (Yamagishi, 1991; McPhie et al., 1993). Although upward gradation to bedded sediments is not exposed, siltstone with subhorizontal lamination filling the space between hyaloclasts and downward gradation of jisaw-fit into coherent lava can be interpreted as sediment infiltration into intra-clast spaces on the exterior of quenched lava bodies (Allen, 1992; Rosa et al., 2010). Because sediment contains marine fossils quench fragmentation of magma occurs most likely in a marine environment. Coherent lava grades everywhere into hyaloclastite breccia suggesting that breccia forms the external carapace of lava flows or domes.

5.3. Massive monomict breccia and megabreccia

Massive monomict breccia is the dominant facies of Los Frailes Formation. Monomict breccia consists of unsorted, clast-supported and structureless breccia with blocks usually less than 1 metre across. Where matrix is present it comprises gravel less than 1cm in diameter. Blocks and matrix gravel are porphyritic and are compositionally identical to coherent lava. Blocks are angular with randomly oriented internal flow banding and many have radially jointed margins. This facies is up to 50 m thick. Where the breccia is in contact with sedimentary units along its base it may include rare rounded phyllite and andesite pebbles. More commonly, the basal contact of this facies is with cross-bedded monomict crystal-rich tuff, and fine-grained material from the tuff is incorporated of the base of the breccia. Discontinous, decimetre-thick beds of breccia

are interbedded with and grading laterally into decimetre thick beds of crystal-rich tuff.

Massive monomict megabreccia is a subfacies of massive monomict breccia characterized by megablocks 1 metre to 20 metres across in coarse-grained matrix of centimetre- to decimetre-size gravel and blocks (Fig. 5D). Megablocks are angular, intact to weakly fractured, with internal flow banding and polyhedral jointing. The contact with matrix is sharp and planar to irregular (Fig. 6A, B). Shear bands are common at the megablock-matrix contact, with shear planes subparallel to the contact and sigmoidal cleavage planes at higher angles to the contact (Fig. 6C). The matrix of megabreccia consists of a clast-supported framework of angular clasts with randomly oriented internal flow banding. Where megabreccia overlies sedimentary units, the base is erosive and characterized by an irregular and discontinuous horizon up to 30 centimetres thick composed of angular to subrounded, millimetre to centimetre-sized dacite lava clasts, together with dense andesite clasts and dacite pumice clasts derived from underlying deposits. These andesite and pumice clasts rapidly disappear upward into the massive megabreccia (Fig. 6D). Monomict megabreccia beds are up to 100 metre thick and grade into massive monomict breccia facies.

5.3.2. Interpretation

A homogeneous primary source for monomict breccia and megabreccia is indicated by monomict angular clasts with randomly oriented flow banding and other clasts present only along the erosive basal contact. Thickness, absence of sorting, massive character, and dominance of angular clasts suggest short transport and rapid en-masse deposition rather than pulsatory events and slow aggradation, while the lack of fine-grained material suggests cohesionless debris flows. Small clasts together with andesite and pumice clasts in discontinuous and thin horizons at the basal contact of

megabreccia facies can be interpreted as clasts ripped up from the substrate due to high basal friction.

The internal structure of massive monomict breccia and megabreccia agree well with the classical description of debris-avalanche deposits, in which megablocks are the "block facies" and centimetre to decimetre-size clasts are the "matrix facies" or "mixed facies" (Glicken, 1991; Palmer et al., 1991; Ui et al., 2001). Monomict character and lack of sorting and internal stratification are consistent with the internal architecture and depositional features of debris-avalanche deposits that result from sector collapse of volcanic edifices (Crandell et al., 1984; Siebert, 1984; Ui and Glicken, 1986; Palmer et al., 1991). Deformation along contacts and fine-grained basal contact are characteristic of debris avalanches and attributed to high shear within the flows (Palmer et al., 1991, Schneider and Fisher, 1998; Ui et al., 2001). We interpret the massive monomict breccia and megabreccia at Los Frailes as deposits of debris avalanches due to lateral collapse of volcanic edifices.

5.4. Diffusely bedded pumice breccia and lapilli tuff

Diffusely bedded pumice breccia and lapilli tuff is a poorly sorted and closely packed aggregate of pumice clasts (65%), dense clasts (15%) and crystals (20%) that shows low-angle and large-scale cross-bedding (Fig. 7A). This facies is dominantly clast supported; where present, matrix (~5%) is altered to sericite containing cuspate, platy, and bubble-wall glass shards (< 0.1 millimetre) and pumice clasts (<0.25 millimetre diameter) with tube vesicles. Pumice clasts are centimetre to decimetre in diameter, subangular to subrounded, occasionally with well-rounded corners, and are often capped by a film up to 1 centimetre thick of millimetre-sized dense clasts and crystals (Fig. 8A). Three types of pumice clasts can be distinguished based on colour,

texture, and composition. White pumices (> 90%) are porphyritic and contain plagioclase (7%), amphibole (5%), biotite (5%), and opaque (1%) phenocrysts in a vesicular groundmass (~70% vesicles) with highly elongated vesicles. Gray pumices (5%) are less vesicular and contain up to 1% clinopyroxene phenocrysts. Banded mingled pumices (5%) consist of an alternation of millimetre-thick bands of white and gray pumice. Dense clasts are ca. 1 centimetre in diameter, subangular, and consist of black to green andesite and amphibole-to biotite-rich dacite. Crystals are plagioclase, amphibole, and biotite. Bedding is laterally diffuse and marked by differences in clast size and by an alternation of centimetre-to decimetre-thick, pumice-rich layers and centimetre-thick layers enriched in dense clasts and crystals (Fig. 9B). Bedding thickness is locally undulatory, with erosional surfaces that become parallel when traced laterally (Fig. 9). Beds of this facies are locally tilted along subhorizontal anastomosed faults, showing small-scale folds and crenulations with axial planes subparallel to fault planes. Fault planes are centimetre-wide zones that truncate bedding at high angles and that are filled with remobilized fine-grained material from the pumice breccia. Pumice clasts in tilted beds are truncated against fault planes, displaying crenulated clast margins and local fiamme-like appearance with the flattening plane subparallel to bedding (Fig. 8B).

5.4.1. Interpretation

Closely packing of blocks and lapilli in a clast-supported framework and poor sorting suggest transport and deposition by gravity-driven granular flows. Rounding of pumice clasts can be attributed to bedload abrasion during transport in hyperconcentrated flows, while films of fines that cap pumice clasts can be interpreted as settling of the finer suspended load. Bedload abrasion in hyperconcentrated flows and

settling of suspended load suggest grain-to-grain and water support mechanisms for the granular flows. Fiamme-like pumice clasts with crenulated margins are local features associated with faulting and remobilization of material along fault planes likely due to high pore pressure. Besides, this facies has a clast-supported framework and rare glass shards within the scarce matrix are not deformed. All these observations argue against fiamme-like clasts produced by primary hot-state welding, and support an origin by flattening of hydrated pumice clasts (cf Gifkins et al., 2005; Bull and McPhie, 2007). Pumice clasts were likely hydrated due to fluid circulation along fault planes.

5.5. Massive pumice to lithic-rich breccia

Massive pumice to lithic-rich breccia is a poorly sorted, clast-supported and non-organized aggregate of lava clasts (45%), pumice clasts (45%), and crystals (10%). Pumice clasts are up to 20 centimetres in diameter and identical to the pumice clasts in the diffusely bedded pumice breccia and lapilli tuff facies. Lava clasts are subangular and up to 40 centimetres in diameter, and are dominantly porphyritic dacite with lesser porphyritic andesite. This facies is up to 3 metres thick and is laterally restricted to less than 15 meters, and grades laterally into diffusely bedded pumice breccia and lapilli tuff (Fig. 7). Lava clasts usually have the largest clast dimension at ca. 15º to the shallower dip angle of the bedding planes in the diffusely bedded pumice breccia and lapilli facies (Fig. 7B).

5.5.1. Interpretation

The clast-supported framework, poor sorting, and gradation into diffusely bedded pumice breccia and lapilli tuff suggest transport and deposition by non-cohesive granular flows. Lack of internal organization can be interpreted as rapid aggradation at the flow boundary zone and the orientation of lava clasts with respect to bedding in the

diffusely bedded pumice breccia and lapilli tuff is likely clast imbrication.

5.6. Massive pumice tuff

Massive pumice tuff is a poorly sorted, matrix-supported and non-organized tuff that contains scattered centimetre-diameter porphyritic dacite lava and pumice clasts and smaller crystals (Fig. 9). The matrix is altered to sericite, and is composed of platy and bubble-wall glass shards (< 0.1 mm in size), pumice clasts (0.1 to 1 mm in size) with tube vesicles and plagioclase crystals. The tuff contains patches and dismembered thin horizons (up to 1 centimetre thick and less than 1 decimetre wide) of fine tuff showing diffuse boundaries and internally distorted fine laminations (Fig. 9B). Porphyritic dacite clasts are subrounded and composed of plagioclase and amphibole with rare pyroxene. Massive pumice tuff is interbedded with diffusely bedded pumice breccia and lapilli tuff (Fig. 9A). It forms tabular bodies up to 50 centimetres thick that extend for 2-3 metres and grade laterally into the diffusely bedded pumice breccia and lapilli tuff. The lower contact of massive pumice tuff is irregular, diffuse and gradational, with pumice clasts from the pumice brecccia mixed with the fine-ash matrix of the massive tuff. The upper contact is convex upward, diffuse to sharp, and truncates the thin horizons of finely laminated tuff in the massive tuff. Beds of the pumice breccia onlap this upper contact, which is usually marked by a lag of dense clasts of the pumice breccia (Fig. 9B).

5.6.1. Interpretation

Massive pumice tuff is intimately related to the diffusely bedded pumice breccia and lapilli tuff facies and the ash matrix is virtually identical in both facies. Tabular geometry of massive pumice tuff together with lateral and downward gradation into

diffusely bedded pumice breccia and lapilli suggests progressive aggradation of granular flows while lack of internal organization indicates steady conditions during sustained deposition (Branney and Kokelaar, 2002). However, the observation that beds of pumice breccia onlap the upper sharp contact and finely laminated horizons suggests different flow units or significant changes in the flow conditions (i.e. flow unsteadiness) in which transport and deposition were primarily dominated by traction processes.

5.7. Cross-bedded monomict crystal-rich tuff

Cross-bedded monomict crystal-rich tuff is a thinly bedded, poorly to well-sorted and fine to very coarse tuff dominantly composed of crystals and crystal fragments, angular porphyritic dacite clasts and minor (< 2%) pumiceous clasts. Crystals are plagioclase, amphibole, biotite and rare pyroxene. Porphyritic dacite consists of plagioclase, amphibole and biotite phenocryst in a glassy groundmass with perlitic cracks and plagioclase microlites. Pumiceous clasts contain plagioclase, amphibole and biotite in a vesicular groundmass (> 40% vesicles) with elongated vesicles. This facies is up to 2 meters thick and shows low angle cross-bedding and cross-lamination, with centimetre- to millimetre-thick, normally and reversely graded beds that display decimetre-spaced scour-and-fill structures (Fig. 10A). Lamination is laterally diffuse and usually distorted by small-scale folds and faults, with fault displacements of millimetres to centimetres.

5.7.1. Interpretation

Grain size, sorting, cross bedding, cross lamination and graded beds with scour and fill structures suggests transport and deposition by traction and turbulence

mechanisms from dilute-granular and water-supported flows. Small-scale faulting and folding of fine lamination can be interpreted as soft-sediment deformation in an aqueous environment.

5.8. Thinly bedded fine tuff

Thinly bedded fine tuff occurs as irregular millimetre to centimetre wide patches within porphyritic dacite lava (Fig. 10B). Patches consist of subhorizontal graded beds with parallel and cross-lamination that is occasionally distorted. Lamination is characterized by an alternation of well-sorted and laterally diffused millimetre-thick horizons that differ in grain size (Fig. 10C). Coarser-size horizons (~0.1 mm grain size) are usually thicker and consist of platy, bubble-shape, and cuspate glass shards, amphibole and plagioclase crystal fragments and rare clasts of undifferentiated porphyritic rock (Fig. 10D). Finer-size horizons (< 0.05 mm grain size) are thinner and consist of an intergrowth of feldspar crystals altered to iron oxides and minor chlorite, with minor glass shards.

5.8.1. Interpretation

Cross-lamination and lateral diffusion of thin horizons indicates transport by traction mechanisms while the marked particle segregation shown by coarser-size and finer-size horizons is characteristic of turbidity-current deposition (Schneider et al., 2001; Gladstone and Sparks, 2002). This facies is interpreted to have been deposited by turbidity currents.

6. Facies architecture and distribution

The Los Frailes Formation is divided into four volcanic units based on the presence of three interbedded sedimentary units that contain marine fossils, which indicate hiatuses in volcanic activity. Coherent lava and hyaloclastite breccia that forms Units 1, 2 and 4 predominate along coastal exposures to the northeast of San José village, to the east of Cerro de Los Frailes, and to the north of the Cerro de Los Frailes (Figs. 2 and 3). Coherent lava and hyaloclastite breccia form lava flows or domes. In most cases the nature of these volcanic bodies cannot be better constrained due to limited exposure, although some outcrops with a tabular geometry suggest lava flow (Fig. 5A).

Massive monomict megabreccia is restricted to inland exposures in Units 2 and 4 to the northeast of San José village and to the south of Cerro de La Palma, where it grades laterally into massive monomict breccia (Fig. 3). Massive monomict breccia is the most widespread lithofacies of the Los Frailes Formation, and makes up volcanic Units 1, 2, and 4. The contacts between massive monomict breccia or megabreccia and the lithofacies forming lava flows or domes have not been observed but these facies are laterally associated in Units 2 and 4 (Fig. 11). For example, Unit 2 is composed of megabreccia subfacies in the Cerro de la Palma stratigraphic log, while less than 1 kilometre to the north in the Casa de la Palma log it is composed of coherent lava that grades upward and downward into hyaloclastite breccia (Fig. 3a). Cross-bedded, monomict crystal-rich tuff is mainly exposed at the base of Units 2 and 4 and grades upward into massive monomict breccia.

Unit 3 is distinctively pumiceous and mainly comprises diffusely bedded pumice breccia and lapilli tuff. To the northeast of San José, this facies is dominated by blocks and is free of fine matrix. The blocks grade upward into lapilli-size clasts, showing persistent planar cross-bedding that indicates paleoflow direction toward the east (Fig.

7). In this area, diffusely bedded pumice breccia and lapilli tuff grades into massive pumice- to lithic-rich breccia in which imbricated dense clasts indicate a paleoflow direction to the southeast. Farther to the northeast at Punta del Esparto, diffusely bedded pumice breccia and lapilli tuff is dominated by lapilli-size clasts with minor ash matrix and is interbedded with massive pumice tuff (Fig. 9). Thinly bedded fine tuff is exposed near Collado de los Grajos (Figs. 2 and 3b); based on the crystal content and the presence of ash-size glass shards, which are similar to those of the diffusely bedded pumice breccia and lapilli and massive pumice tuff, this fine tuff is considered part of Unit 3. Thinly bedded fine tuff occurs toward the top of lava flow or dome facies of Unit 2 on poorly exposed outcrops and upward gradation to bedded sediments is not observed. Nevertheless, preservation of subhorizontal lamination of the tuff may suggest sediment infiltration into fractured dacite lava.

7. Discussion

7.1. Depositional environment of debris avalanche deposits at Los Frailes and comparison with other examples

Several of the textural characteristics of the fragmental facies in the Los Frailes Formation can be reconciled with the subaqueous emplacement of debris avalanches produced by sector collapse of submarine lava flows and domes. The largely monomictic composition of all breccias and the presence of dikes of the same composition suggest a local origin from a lava flow or dome complex. Lateral association of breccia and megabreccia facies with coherent lava grading into outward carapace of hyaloclastite breccia suggests a depositional environment associated with subaqueous lava flows or domes (Figs. 3b and 11). Radially jointed clasts in massive

monomict breccia are similar to the pseudo-pillows and lava lobes surrounded by hyaloclastite breccia in subaqueous lava flows and domes (Yamagishi, 1991; Goto and Tsuchiya, 2004). Hence, mass wasting of the external hyaloclastite breccia carapace may have provided material for the "matrix facies" of the debris avalanche, while internal coherent portions provided megablocks of the "block facies". Nevertheless, clast production due to dynamic disintegration during transport is characteristic of debris avalanche deposits and cannot be excluded (Crandell et al., 1984; Voight et al., 1983; Glicken et al., 1991). Breccia and megabreccia facies are interbedded with carbonate sediments that contain marine fossils, indicating a marine depositional environment.

Sector collapse of volcanic edifices produce debris avalanches with variable facies, facies distributions, thicknesses, volumes, run-out distances, clast sizes and clast fracturing, all of which are strongly dependent on the structure of the source area and the physiographic features along transport (Palmer et al., 1991; Voight et al., 2002). Most of the examples of subaqueous debris avalanches in the literature are Quaternary; to our knowledge, just one example describes an ancient (Archean) submarine debris avalanche (Trofimovs et al., 2004). Based on the scale of the debris avalanche (i.e. volume, extension and run-out distance), three groups can be broadly distinguished. Debris avalanches caused by sector collapse of ocean-island volcanoes like Hawaii and the Canary Islands are large-scale events (volume > 100 km^3, area > 1000 km^2, run-out ~ 100 km) that accumulate volcanic debris on the sea floor (Moore et al., 1989; Masson et al., 2002). Lateral collapse of stratovolcanoes like Mount St. Helens, Mount Shasta and Colima are less voluminous and extended (volume < 50 km^3, area < 500 km^2) and their run-out distance is usually less than 100 km (Crandell et al., 1984; Voight et al., 1983; Stoopes and Sheridan, 1992). Sector collapse of volcanic domes like Unzen,

Montserrat, Mount St. Augustine and Cerro Pizarro are small-scale processes of volume < 1 km^3, area < 20 km^2 and run-out distance < 10 km (Beget and Kienle, 1992; Ui et al., 2001; Voight et al., 2002; Riggs and Carrasco-Núñez, 2004).

Recognition of the source area for the Los Frailes debris avalanche deposits is difficult due to erosion of the original volcanic edifices and emplacement of overlying stratigraphic units (the Cerro de La Palma Formation). However, based on exposed thickness, extension and lateral association of debris-avalanche deposits with coherent lava and hyaloclastite breccia, very rough estimates of their volume, extension, and runout distance can be made. Considering the maximum thickness of massive monomict megabreccia (100 meters), that it grades laterally into much thinner (< 50 meters) massive monomict breccia, and taking the areal distribution of both facies, a volume of less than 0.5 km^3, an area of less than 10 km^2 and a run-out distance of less than 5 km can be approximated for the debris avalanche deposits of Unit 2. Debris avalanche deposits of Unit 4 are probably less voluminous and with shorter runout distance. The scale of the Miocene debris avalanche deposits at Los Frailes is similar to those that result from sector collapse of volcanic domes in Quaternary examples. However, the maximum thickness of megabreccia facies in Los Frailes is thicker than the usual thickness of debris avalanche deposits by sector collapse of domes in Quaternary examples, suggesting that avalanches at Los Frailes were likely confined within valleys.

7.2. Facies model and volcanic evolution of the Los Frailes Formation

The Los Frailes Formation has been interpreted as a dome complex erupted in a shallow-water environment (Fernández Soler, 1987) and as a resurgent collapse caldera that formed close to sea level (Cunningham et al., 1990). In the latter interpretation,

Unit 3 of Los Frailes Formation is thought to be the caldera-forming eruption and some of the lithofacies of this unit are interpreted as welded tuffs. However, as stated above, fiamme-like pumice clasts are better interpreted as flattening of hydrated pumice clasts rather than primary hot-state welding. Rhyolite tuffs of the Casa del Tomate Formation and of the Rodalquilar Group were mistaken for dacitic pumiceous deposits of Unit 3 by Cunningham et al. (1990) providing an overestimation on the volume eruption. The lithofacies and observations provided here on pumiceous deposits of Unit 3 are more in agreement with a low-volume eruption rather than with a caldera-forming eruption.

Distinguishing between eruption-fed and remobilized volcaniclastic deposits may not always be possible and is far more difficult when dealing with ancient successions (White, 2000; Schneider et al., 2001; Walker et al., 2008). Volcaniclastic deposits in the Los Frailes Formation might not be strictly eruption-fed (i.e. by primary eruptions). However, volcanic units are clearly bounded by sedimentary units that indicate periods of volcanic quiescence and volcaniclastic deposits are laterally associated with coherent lava grading into hyaloclastite breccia (Figs. 3b and 11). For these reasons we assume that they were deposited during volcanic cycles contemporaneous with volcanic activity, although not necessarily fed by primary eruptions.

Phenocrysts phases of volcanic and volcaniclastic rocks of the Los Frailes Formation and most dikes in Los Frailes area are similar and major elements show a homogeneous composition (Fig. 4). This similarity, together with the areal distribution of lithofacies and dikes suggest similar magma sources that evolved very little through time. The chemical composition of white pumice in Unit 3 corresponds to a more evolved magma than Units 2 and 4 (Fig. 4).

A megablock in debris-avalanche deposits of Unit 2 yielded an age of 12.71 Ma

and dikes of the Los Frailes Formation intrude rhyolite tuff of the Casa del Tomate Formation (dated at 12.13 Ma), suggesting that volcanism of the Los Frailes Formation was still active after the tuff emplacement. Given that Unit 1 of Los Frailes underlies Unit 2, the volcanic activity of the Los Frailes Formation may have encompassed less than 1 Ma, comprising periods of volcanic quiescence, erosion and sediment deposition, and periods of volcanic growth and contemporaneous mass wasting. Two different arrays shown by trace elements of rocks from the Los Frailes Formation and Cerro la Palma Formation and a hiatus of ~3 Ma between these units suggest differentiation from different parental magmas. During emplacement of Units 1, 2, and 4, volcanic activity was effusive eruption of lava and concurrent episodes of sector collapse that produced debris-avalanches deposits. Unit 3, which contains ash shards and pumice clasts in diffusely bedded pumice breccia and tuff, massive pumice tuff and thinly bedded fine tuff lithofacies, represents explosive activity that likely produced low-volume pyroclastic flows. Although the depositional environment for these facies is subaqueous, eruption of pyroclastic flows from subaerial vents cannot be excluded.

8. Conclusions

The Los Frailes Formation consists of thick intervals of volcanic and volcaniclastic rocks interbedded with thinner intervals of sedimentary rocks that were deposited during periods of volcanic repose. Contacts between volcanic and sedimentary intervals are discordant and erosive. This succession is divided into formal lithostratigraphic units based on lithology, composition, and stratigraphic position. Volcanic rocks are two-pyroxene calc-alkaline rocks that range in composition from basaltic andesite to rhyolite, with dacite being the most abundant. $^{40}Ar/^{39}Ar$ dating of

volcanic rocks from different units together with interbedded carbonate sediments reveal hiatuses in the volcanic activity.

Lithofacies of the Los Frailes Formation comprise dacite lava and volcaniclastic facies, including different types of volcanic breccias and tuffs, interbedded with sedimentary strata. Hyaloclastite breccia that grades into coherent lava and shallow-water marine fossils in sedimentary strata suggest a submarine depositional environment. Massive monomict brecia and megabreccia are typical of volcanic debris avalanche deposits. Deformation at the megablock-matrix contact and fine-grained basal contacts in massive monomict breccia and megabreccia are characteristic of debris avalanches and attributed to high shear during transport. Monomict character and the lateral association of breccia and megabreccia facies with coherent lava grading into outer carapace of hyaloclastite breccia suggest that debris avalanches were produced by sector collapse of submarine lava flows and domes. Despite limited exposure due to erosion and emplacement of overlying units, rough estimates of the volume (< 0.5 km^3), area (< 10 km^2) and run-out (< 5 km) of debris avalanches at Los Frailes are in agreement with those in Quaternary examples that are inferred to be due to sector collapse of volcanic domes.

The volcanic activity of the Los Frailes Formation may have encompassed less than 1 m.y., comprising periods of volcanic quiescence, erosion and sediment deposition, and cycles of volcanic growth and contemporaneous mass wasting. Most volcanic units of the Los Frailes Formation were emplaced by effusive volcanic activity, and repeated mass wasting events produced debris avalanches by sector collapse of domes. Low-volume explosive volcanism likely caused emplacement of pyroclastic flows as suggested by ash shards and pumice clasts in diffusely bedded pumice breccia and lapilli tuff, massive pumice-tuff and thinly bedded fine tuff.

Acknowledgements

This research was funded by projects CGL2005-03511/BTE, HI2006-0073 and CGL2009-06968-E from the Ministerio de Ciencia e Innovación of Spain. Chemical analyses were performed with the financial support of Italian MIUR – PRIN 2008 funds, and grant # 2008HMHYFP_002 issued to Conticelli. Dr. Luigi Franciosi (Naples) is warmly thanked for allowing access to XRF facilities, as is Alia Jasim for carrying out some chemical analyses. Brian Jicha did $^{40}Ar/^{49}Ar$ analyses and has our thanks for doing this work and helping us interpret the results. J.M. Fernández Soler shared with us of his PhD thesis. Antonio Vázquez helped with identification of marine fossils. We thank the Parque Natural Cabo de Gata-Níjar for giving us permission to undertake this research. We also thank the participants of the Workshop held in May, 2011 (http://www.ija.csic.es/cabodegata/) for fruitful discussions in the field. Careful reviews by Jean-Luc Schneider and Alexander Belousov greatly improved the manuscript and are much appreciated.

References

Allen, R.L. 1992. Reconstruction of the tectonic, volcanic and sedimentary setting of strongly deformed Zn-Cu massive sulfide deposit at Benambra, Victoria. Economic Geology 87, 825-854.

Arribas, A. 1993. Mapa Geológico del Distrito Minero de Rodalquilar. IGME.

Beget, J.E. and Kienle, J. 1992. Cyclic formation of debris avalanches at Mount St Augustine volcano. Nature 356, 701-704.

Benito, R., López-Ruiz, J., Cebriá, J.M., Hertogen, J., Doblas, M., Oyarzun, R.,

Demaiffe, D., 1999. Sr and O isotope constraints on source and crustal contamination in the high-K calc-alkaline and shoshonitic Neogene volcanic rocks of SE Spain. Lithos 46, 773-802.

Branney, M.J. and Kokelaar, P. 2002. Pyroclastic Density Currents and the Sedimentation of Ignimbrites. Geological Society, London, Memoirs, 27.

Bull, K.F. and McPhie, J. 2007. Fiamme textures in volcanic successions: Flaming issues of definition and interpretation. Journal of Volcanology and Geothermal Research 164, 205-216.

Cas, R.A.F., Allen, R.F., Bull, S.W., Clifford, B.A., and Wright, J.V. 1990. Subaqueous, rhyolitic dome-top tuff cones: A model based on Devonian Bunga Beds, southeastern Australia and a modern analogue. Bulletin of Volcanology 52, 159-174.

Chadwick Jr., W.W., Wright, I.C. Schwartz-Schampera, U., Hyvernaud, O., Reymond, D., de Ronde C.E.J. 2008. Cyclic eruptions and sector collapses at Monowai submarine volcano, Kermadec arc: 1998-2007. Geochemistry Geophysics Geosystems 9, 1-17.

Conticelli, S., Guarnieri, L., Farinelli, A., Mattei, M., Avanzinelli, R., Bianchini, G., Boari, E., Tommasini, S., Tiepolo, M., Prelević, D., Venturelli, G., 2009a. Trace elements and Sr-Nd-Pb isotopes of K-rich, shoshonitic, and calc-alkaline magmatism of the Western Mediterranean Region: genesis of ultrapotassic to calc-alkaline magmatic associations in a post-collisional geodynamic setting. Lithos 107, 68-92.

Crandell, D.R., Miller, C.D:, Glicken, H.X, Christiansen, R.L. and Newhall, C.G. 1984. Catastrophic debris avalanche from ancestral Mount Sashta, California, Geology 12, 143-146.

Cunningham, C. G., Arribas, A. Jr., Rytuba, J.J., Arribas, A. 1990. Mineralized and unmineralized calderas in Spain; Part 1, evolution of the Los Frailes caldera. Mineralium Deposita v. 25 (supp.), S21-S28.

De Rita, D., Giordano, G. and Cecili, A. 2001. A model for submarine rhyolite dome growth: Ponza Island (central Italy). Journal of Volcanology and Geothermal Research 107, 221-239.

Dewey, J.F., Helman, M.L., Turco, E., Hutton, D.H.W., Knott, S.D., 1989. Kinematics of the Western Mediterranean. In: Coward, M.P., Dietrich, D., Park, R.G.(Eds.), Alpine Tectonics, Geological Society of London, Special Publication, 45, 265-283.

Di Battistini, G., Toscani, L., Iaccarino, S., Villa, I.M. 1987. K/Ar ages and the geological setting of calc-alkaline volcanic rocks from Sierra de Gata, SE Spain. Neues Jahrbuch für Mineralogie, Monatshefte H. 8, 369-383.

Doblas, M., López-Ruiz, J., Cebriá, J.-M., 2007. Cenozoic evolution of the Alborán domain: a review of the tectonomagmatic models. In: "Cenozoic Volcanism in the Mediterranean Area", L. Beccaluva, G. Bianchini, M. Wilson (edts), The Geological Society of America, Special Papers, 418, 303-320.

Duggen, S., Höernle, K., van den Bogaard, P., Garbe-Schönberg, D., 2005. Post-collisional Transition from subduction-to intraplate-type magmatism in the westernmost Mediterranean: Evidence for Continental-Edge Delamination of subcontinental lithosphere. Journal of Petrology 46, 1155-1201.

Fernández Soler., J.M. 1987. Análisis e interpretación de los materiales volcánicos del Cerro de los Frailes (Cabo de Gata, Almería). Estudios Geológicos 43, 359-366.

Fernández-Soler., J.M. 2001. Volcanics of the Almeria Province. In Mather, A., Martin,

J.M., Harvey, A., Braga, J. (Eds.) A field guide to the Neogene Sedimentary Basins of the Almeria Province, South-East Spain. IAS Field Guide Blackwell Science, Oxford, UK, pp 58-88.

Fiske, R.S. and Matsuda, T. 1964. Submarine equivalents of ash flow tuffs in the Tokiwa Formation, Japan. American Journal of Science 262, 76-106.

Fiske, R.S., Naka, J., Iizas, K., Yuasa, M. and Klaus, A. 2001. Submarine silicic caldera at the front of the Izu-Bonin arc, Japan: voluminous seafloor eruptions of rhyolite pumice.Geololgical Society of America Bulletin 113, 813-824.

Fuster, J.M., Aguilar, M.J., García, A. 1965. Las sucesiones volcánicas en la zona del Pozo de los Frailes dentro del vulcanismo cenozoico del Cabo de Gata (Almería). Estudios Geológicos XXI, 199-222.

Gifkins, C.C., Allen, R.L. and McPhie, J. 2005: Apparent welding textures in altered pumice-rich rocks. Journal of Volcanology and Geothermal Research 142, 29-47.

Gladstone, C. and Sparks, R.S.J. 2002. The significance of grain-size breaks in turbidites and pyroclastic density current deposits. Journal of Sedimentary Research 72, 182-191.

Glicken, H. 1991. Sedimentary architecture of large volcanic-debris avalanches. In Sedimentation in Volcanic settings. SEPM Special Publication 45, 99-106.

Goto, Y. and Tsuchiya, N. 2004. Morphology and growth style of a Miocene submarine dacite lava dome at Atsumi, northeast Japan. Journal of Volcanology and Geothermal Research 134, 255-275.

Johnson, C.L., Franseen, E.K. and Goldstein, R.H. 2005. The effects of sea level and

paleotopography on lithofacies distribution and geometries in hetereozoan carbonates, south-eastern Spain. Sedimentology 52, 513-536.

Kano K., Yamamoto T., and Ono K., 1996. Subaqueous eruption and emplacement of the Shinjima Pumice, Shinjima (Moeshima) Island, Kagoshima Bay, SW Japan, . Journal of Volcanology and Geothermal Research 71, 187-206.

Leat, P.T., Tate, A.J., Tappin, D.R., Day, S.J. and Owen, M.J. 2010. Growth and mass wasting of volcanic centers in the northern South Sandwich arc, South Atlantic, revealed by new multibeam mapping. Marine Geology 275, 110-126.

Martín, J.M., Braga, J.C., Betzler, C. and Brachert, T.C. 1996. Sedimentary model and high-frequency cyclicity in a Mediterranean, shallow-shelf, temperate-carbonate environment (uppermost Miocene, Agua Amarga Basin, Southern Spain). Sedimentology 43, 263-277.

Masson, D.G., Watts, A.B., Gee, M.J.R., Urgeles, R., Mitchell, N.C., Le Bas, T.P. and Canals, M. 2002. Slope failures on the flanks of the western Canary Islands. Earth Science Reviews 57, 1-35.

McPhie, J., Doyle, M. And Allen, R.L. 1993. Volcanic Textures: a guide to the interpretation of textures in volcanic rocks. Centre for Ore Deposit and Exploration Studies, University of Tasmania, Hobbart.

Montenat, C. and Ott d'Estevou, Ph. 1990. Eastern Betic Neogene basins-A Review. Doc. Et Trav. Igal. 12-13, 9-15.

Moore, J.G., Clague, D.A., Holcomb, R.T., Lipman, P.W., Normark, W.R. and Torresan, M.E. 1989. Prodigious submarine landslides in the Hawaiian ridge. Journal of

Geophysical Research 94, 17,465-17,484.

Palmer, B.A., Alloway, B.V. and Neall, V.E. 1991. Volcanic-debris-avalanche deposits in New Zealand-Lithofacies organization in unconfined, wet-avalanche flows. In Sedimentation in Volcanic settings. SEPM Special Publication 45, 89-98.

Pichler, H. 1965. Acid hyaloclastites. Bulletin of Volcanology 28, 293-310.

Prelević, D., Foley, S.F., Romer, R.L., Conticelli, S., 2008. Mediterranean Tertiary Lamproites: Multicomponent melts in post-collisional geodynamics. Geochimica et Cosmochimica Acta 72, 2125-2156.

Reicherter, K. and Hübscher, C. 2007. Evidence for a sea floor rupture of the Carboneras Fault Zone (southeastern Spain): Relation to the 1522 Almeria earthquake? Journal of Seismology 11, 15-26.

Riggs, N. and Carrasco-Núñez, G. 2004. Evolution of a complex isolated dome system, Cerro Pizarro, central México. Bulletin of Volcanology 66, 322-335.

Rosa, C.J.P., McPhie, J. and Relvas, J.M.R.S. 2010. Type of volcanoes hosting the massive sulfide deposits of the Iberian Pyrite Belt. Journal of Volcanology and Geothermal Research 194, 107-126.

Sáenz de Galdeano, C. and Vera, J.A. 1992. Stratigraphic record and palaeogeographical context of the Neogene basins in the Betic Cordillera. Basin Research 4, 21-36.

Schneider, J.-L. and Fisher, R.V. 1998. Transport and emplacement mechanisms of large volcanic debris-avalanches: evidence from the northwest sector of the Cantal Volcano (France). Journal of Volcanology and Geothermal Research 83, 141-165.

Schneider, J.-L., Le Ruyet, A., Chanier, F., Buret, C., Ferrière, J., Proust, J.-N. and Rousseel, J-B. 2001. Primary or secondary distal turbidites: how to make the distinction? An example from the Miocene of New Zealand (Mahia Peninsula, North Island). Sedimentary Geology 145, 1-22.

Siebert, L. 1984. Large volcanic debris avalanche: characteristics of source areas, deposits and associated eruptions. Journal of Volcanology and Geothermal Research 22, 163-197.

Scotney, P. Burgess, R. and Rutter, E.H., 2000. $^{40}Ar/^{39}Ar$ age of the Cabo de Gata volcanic series and displacements on the Carboneras fault zone, SE Spain. Journal of the Geological Society, London 157, 1003-1008.

Serrano, F. Biostratigraphic control of Neogen volcanism in Sierra de Gata (south-east Spain). Geologie en Mijnbow 71, 3-14.

Stoopes, G.R. and Sheridan, M.F. 1992. Giant debris avalanche from the Colima Volcanic Complex, México, implications for long runout landslides (>100 km) and hazard assessment. Geology 20, 299-302.

Tommasini, S., Avanzinelli, R., Conticelli, S., 2011. The Th/La and Sm/La conundrum of the Tethyan realm lamproites. Earth and Planetary Science Letters 301, 469-478.

Torres-Roldán, R.L., Poli, G. and Peccerillo, A., 1986. An early Miocene arc-tholeiitic magmatic dike event from the Alboran Sea -Evidence for precollisional subduction and back-arc crustal extension in the westernmost Mediterranean. Geologische Rundschau 75, 219-234.

Trofimovs, J., Cas, R.A.F. and Davis, B.K. 2004. An Archean submarine volcanic

debris avalanche deposit, Yilgarn Craton, western Australia, with komatiite, basalt and dacite megablocks. The product of dome collapse. Journal of Volcanology and Geothermal Research 138, 111-126.

Trofimovs, J., Amy, L., Boudon, G., Deplus, C., Doyle, E., Fournier, N., Hart, M.B., Komorowski, J.C., Le Friant, A., Lock, E.J., Pudsey, C., Ryan, G., Sparks, R.S.J. and Talling, P.J. 2006. Submarine pyroclastic deposits formed at Soufrière Hills volcano, Montserrat (1995-2003): What happens when pyroclastic flows enter the ocean? Geology 34, 549-552.

Turner, S.P., Platt, J.P., George, R.M.M., Kelley, S.P., Pearson, D.G., Nowell, G.M., 1999. Magmatism associated with orogenic collapse of the Betic-Alborán domain, SE Spain. Journal of Petrology 40 1011-1036.

Ui, T. and Glicken H.X. 1986. Internal structural characteristics of debris avalanche from Mount Sahsta, California, U.S.A. Bulletin of Volcanology 48, 189-194.

Ui, T., Takarada, S. and Yoshimoto, M. 2001. Debris avalanches. In: Sigurdsson H. (Ed.) Encyclopedia of volcanoes. Academic Press, San Diego, 617-626.

Venturelli, G., Capedri, S., Di Battistini, G., Crawford, A.J., Kogarko, L.N., Celestini, S., 1984. The ultrapotassic rocks fron souteastern Spain. Lithos 17, 37-54.

Voight, B., Janda, R.J., Glicken, H.X. and Douglass, P.M. 1983. Nature and mechanics of the Mount St-Helens rockslide-avalanche of 18 May 1980. Geotechnique 33, 243-273.

Voight, B., Komorowski, J.C., Belusov, A.B.; Belusova, M., Boudon, G., Francis, P.W., Franz, V., Heinrich, P., Sparks, R.S.J., and Young, S.R. 2002. The 26 December

(Boxing Day) 1997 sector collapse and debris avalanche at Soufrière Hills Volcano, Montserrat. In: Druitt, T.H. and Kokelaar, B.P. (Eds.) The eruption of Soufrière Hills Volcano, Montserrat, from 1995-1999. Geological Society London Memoir 21, 363-407.

Walker, S.L., Baker, E.T., Resing, J.A., Chadwick Jr., W.W., Lebon, G.T., Lupton, J.E., and Merle, S.G. 2008. Eruption-fed particle plumes and volcaniclastic deposits at a submarine volcano: NW Rota-1, Mariana Arc: Journal of Geophysical Research 113, B08S11

White, J.D.L. 2000. Subaqueous eruption-fed density currents and their deposits. Precambrian Research 101, 87-109.

White, J.D.L., Smellie, J.L. and Clague, D.A. (Eds) 2003, Submarine Explosive Volcanism. Monograph, 140, American Geophysical. Union., p. 379.

Wright, I.C. 2001. In situ modification of modern submarine hyaloclastic/pyroclastic deposits by oceanic currents: an example from the southern Kermadec arc (SW Pacific). Marine Geology 172, 287-307.

Yamagishi, H. 1991. Morphological and sedimentological characteristics of the Neogene submarine coherent lavas and hyaloclastites in Southwest Hokkaido, Japan. Sedimentary Geology 74, 5-23.

Yamagishi, H. and Dimroth, E. 1985. A comparison of Miocene and Archean rhyolite hyaloclastites: evidence for a hot and fluid rhyolite lava. Journal of Volcanology and Geothermal Research 23, 337-355.

***Revision, changes marked**

Click here to view linked References

Dear Prof. Wilson,

Most of the changes have been directly done in the revised version. In most cases they correspond to English grammar and style which has been fully reviewed by the English speaking author Nancy Riggs. So, we please refer you and the reviewers to this new version.

Yours sincerely,

Carles

Table

Click here to download high resolution image

ICS		Fúster et al. (1965)	Bordet (1985)	Fernández Soler (1987)	Cunningham et al. (1990)	Serrano (1992)	This work
Miocene	Tortonian	Tortonian dacites	Cycle C	Frailes-II	Post-Caldera	Coastal Volcanoes	Cerro de la Palma Fm Casa del Tomate Fm
	11.608 Ma	Helvetian pyroxene andesites	Cycle B_2				
		Burdigalian amfibolic andesites	Cycle B_1	Frailes-I	Syn-Caldera	Group B	Los Frailes Fm
	Serravalian	Pre-Burdigalian andesites	Cycle A	Pre-Frailes	Pre-Caldera	Group A	Caliguera Fm

Table 1

Table

Click here to download Table: Table 2.xls

Summary of $^{40}Ar/^{39}Ar$ incremental heating experiments

						Weighted Mean Analysis				Isochron Analysis		
Sample	Rock type	Unit	Location	Material	K/Ca total	^{39}Ar %	MSWD	Age (Ma) ± 2 σ	N	$^{40}Ar/^{36}Ar$ ± 2 σ	MSWD	Age (Ma) ± 2 σ
CG307	coherent lava	Cerro de la Palma Fm	36°46'28.50"N 2° 5'24.36"W	groundmass	0.192	89.3	1.92	**9.32 ± 0.07**	8 of 10	291.8 ± 8.2	1.86	9.35 ± 0.11
CG352	pumice tuff	Casa del Tomate Fm	36°46'40.26"N 2°04'11.94"W	plagioclase	0.064	61.2	0.82	**12.13 ± 0.20**	7 of 10	309.7 ± 55.8	0.93	12.04 ± 0.41
CG308	megablock in megabreccia	Unit 4 of Los Frailes Fm	36°46'25.02"N 2° 5'26.40"W	groundmass	1.459	65.0	0.66	**12.42 ± 0.04**	7 of 10	290.7 ± 5.5	0.19	12.55 ± 0.15
CG309	megablock in megabreccia	Unit 2 of Los Frailes Fm	36°46'11.40"N 2° 5'39.48"W	groundmass	0.744	91.4	0.43	**12.71 ± 0.09**	7 of 10	295.7 ± 1.4	0.50	12.70 ± 0.11

All ages calculated using the decay constants of Steiger and Jäger ($\lambda_{40K} = 5.543 \times 10^{-10}$ yr^{-1})
J-value calculated relative to 28.34 Ma for the Taylor Creek sanidine
Age in **bold** is preferred

Table
Click here to download Table: Table 3.doc

Table 3. Volcanic lithofacies of Los Frailes Formation

Lithofacies	Description	Association with other lithofacies	Interpretation
Coherent lava	Porphyritic, flow banded, columnar jointed. Amygdules and spherulites in groundmass. Up to 40 m thick	Grades into hyaloclastite breccia. Laterally associated with massive monomict breccia and megabreccia	Lava flow or dome
Hyaloclastite breccia	Monomict, clast to matrix supported. Subequant and subangular clasts with curviplanar edges. Jigsaw fit and slight rotation of clasts. About 40 m thick	Grades into coherent lava. Laterally associated with massive monomict breccia and megabreccia	Subaqueous quench fragmentation of magma. External carapace of lava flow or dome
Massive monomict breccia *Subfacies* Massive monomict megabreccia	Unsorted, clast-supported. Angular clasts with flow banding randomly oriented. Up to 50 m thick. Erosive base Blocks up to 20 m across in a coarse matrix. Sharp block/matrix contact with shear-cleavage structures. Erosive base. Up to 100 m thick	Grades laterally into massive monomict megabreccia subfacies. Overlies cross-bedded monomict crystal-rich tuff	Debris avalanche deposits due to sector collapse of lava flow or dome
Diffusely bedded pumice breccia and lapilli tuff	Poorly sorted, clast-supported and closely packed aggregate. Pumice, dense clasts, crystals and minor bubble-wall shards. Up to 40 m thick	Grades into massive pumice to lithic-rich breccia and into massive pumice tuff	Syn-eruptive gravity-driven granular flow
Massive pumice to lithic-rich breccia	Poorly sorted, clast supported and closely packed aggregate. Dense clasts, pumice and crystals. Local imbrication of dense clasts. Up to 3 m thick	Grades into diffusely bedded pumice breccia and lapilli tuff	Syn-eruptive gravity-driven granular flow
Massive pumice tuff	Poorly sorted and matrix supported. Pumice and dense rocks clasts in an ash-size matrix of bubble-wall shards. Up to 0.5 m thick	Grades down and laterally into diffusely bedded pumice breccia and lapilli tuff. Erosive upper contact with diffusely bedded pumice breccia and lapilli tuff	Syn-eruptive gravity-driven granular flow
Cross-bedded monomict crystal-rich tuff	Thinly bedded, poorly to well-sorted, very coarse. Graded beds, soft-sediment deformation. Up to 2 m thick	Overlain by massive monomict breccia	Syn-eruptive dilute granular flow
Thinly bedded fine tuff	Well-sorted, cross-laminated. Platy and bubble-wall shards and minor crystals. Lamination is mm thick, laterally diffuse and distorted	Irregular patches and veins within fractured and brecciated lava toward the base of flow or dome	Syn-eruptive turbidity current deposition. Subsequent fluidization and injection of tuff at the base of lava flow or dome

Figure

Click here to download high resolution image

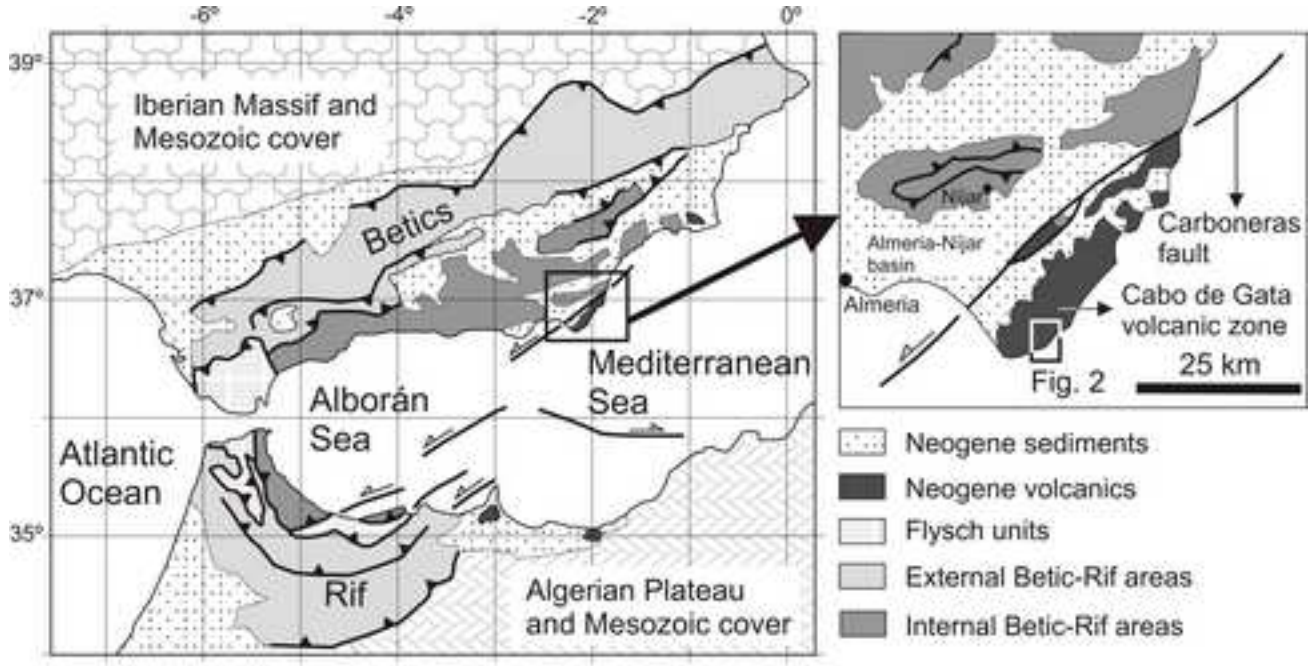

Fig. 1

Figure

Click here to download high resolution image

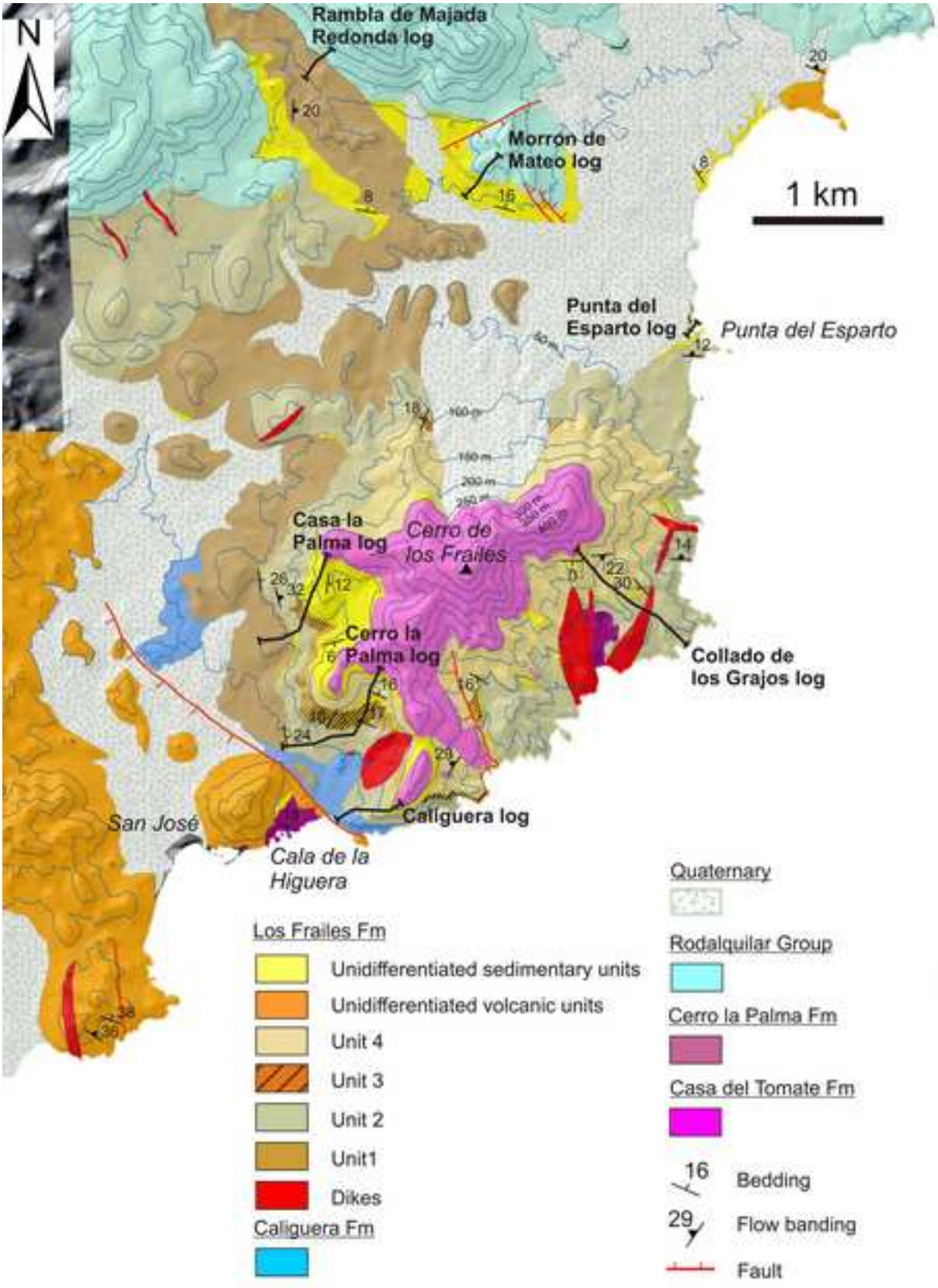

Fig. 2

Figure

Click here to download high resolution image

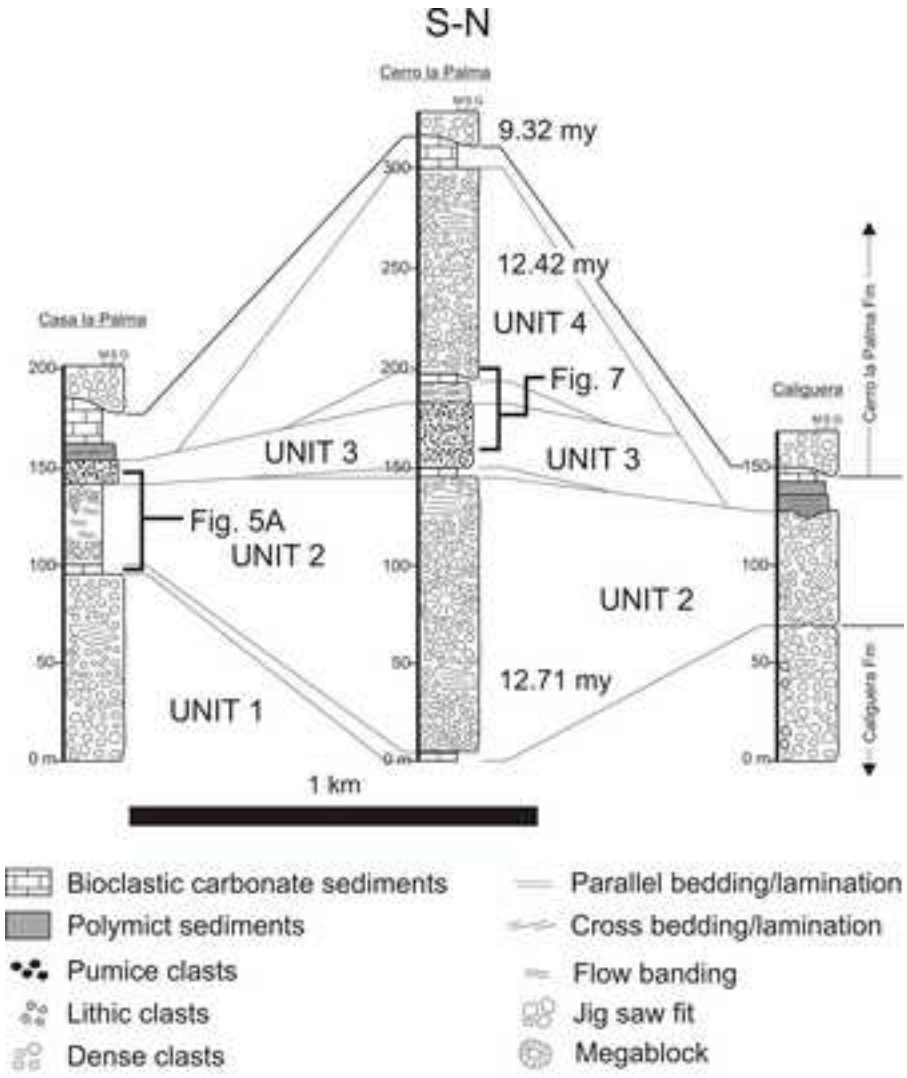

Fig. 3a

Figure

Click here to download high resolution image

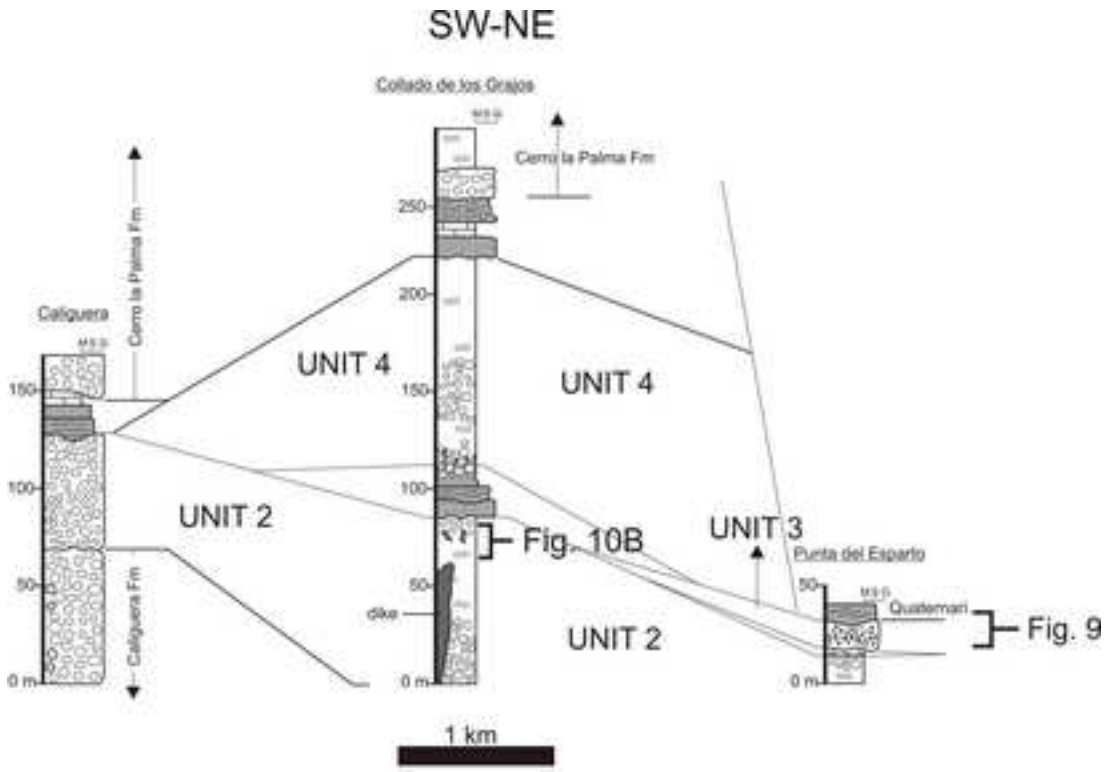

Fig. 3b

Figure

Click here to download high resolution image

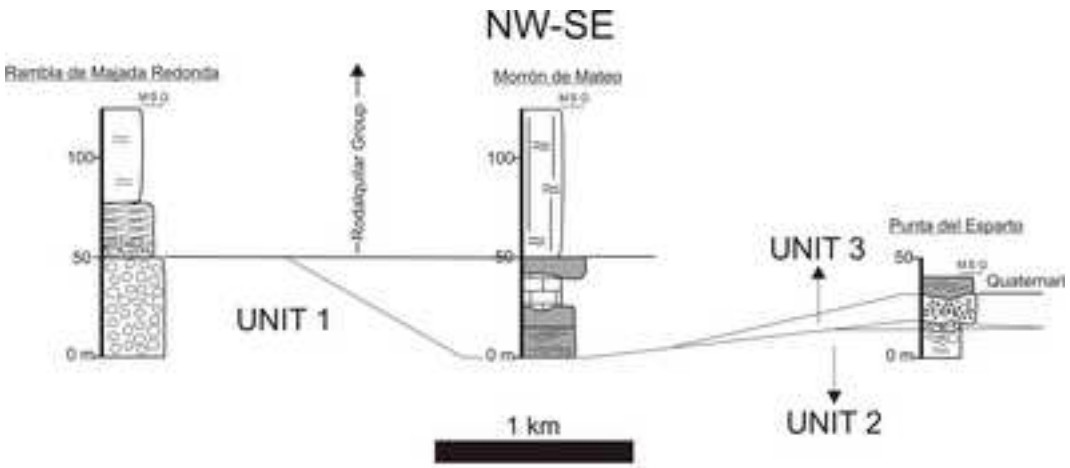

Fig. 3c

Figure

Click here to download high resolution image

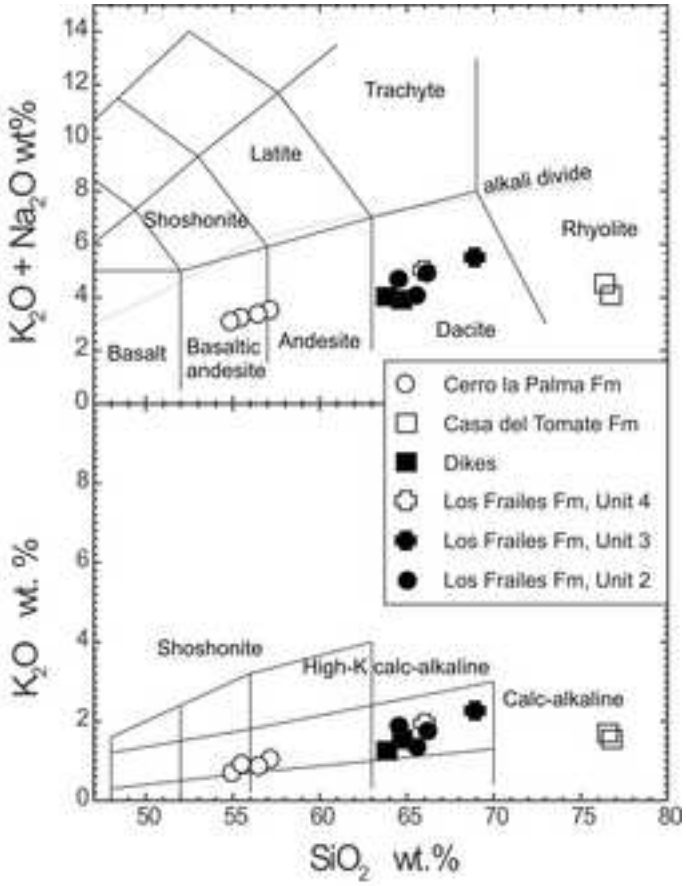

Fig. 4

Figure
Click here to download high resolution image

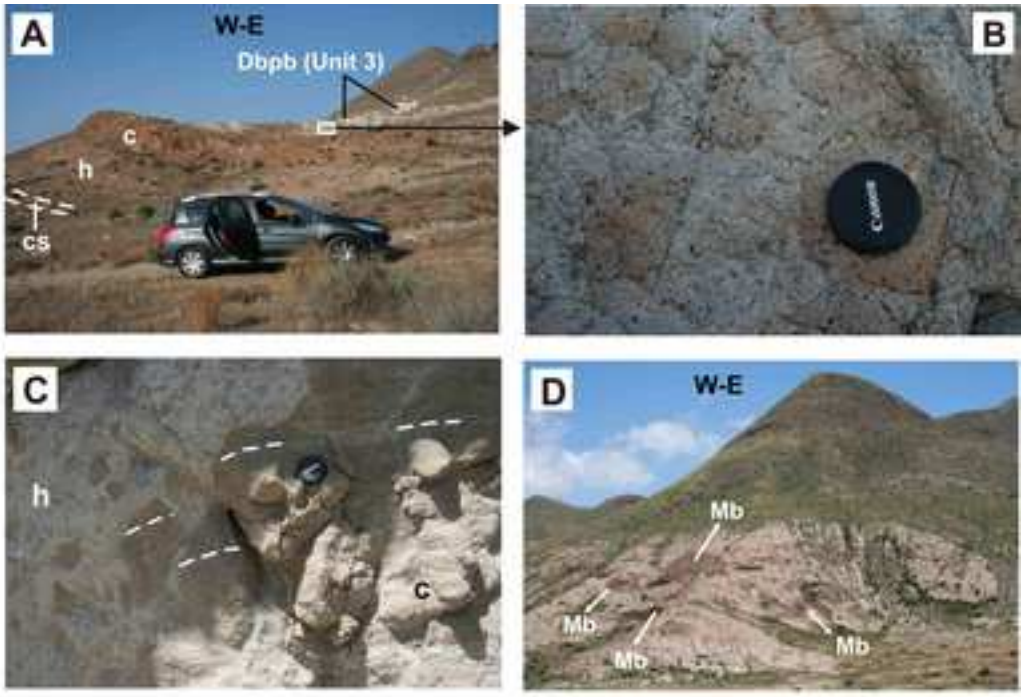

Fig. 5

Figure

Click here to download high resolution image

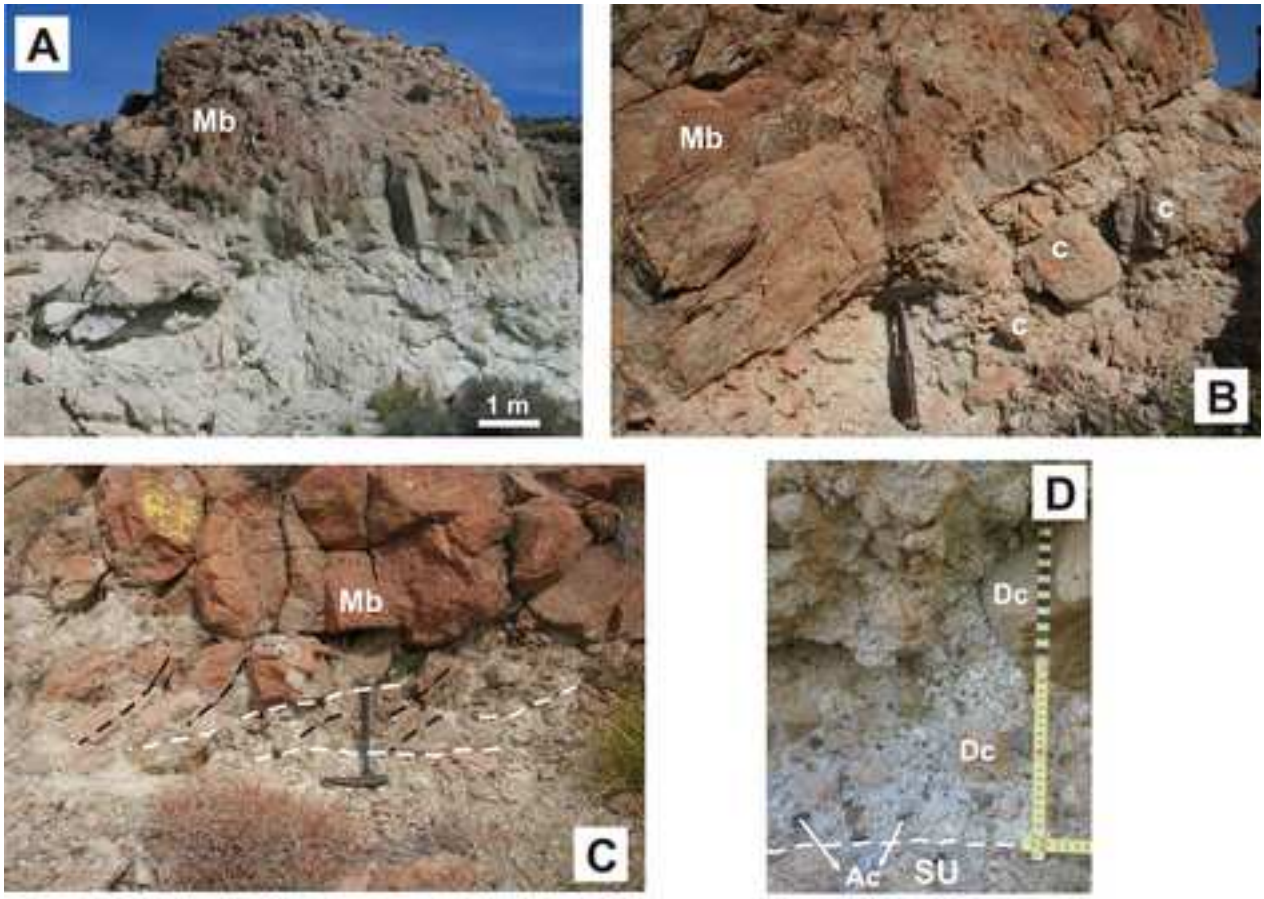

Fig. 6

Figure

Click here to download high resolution image

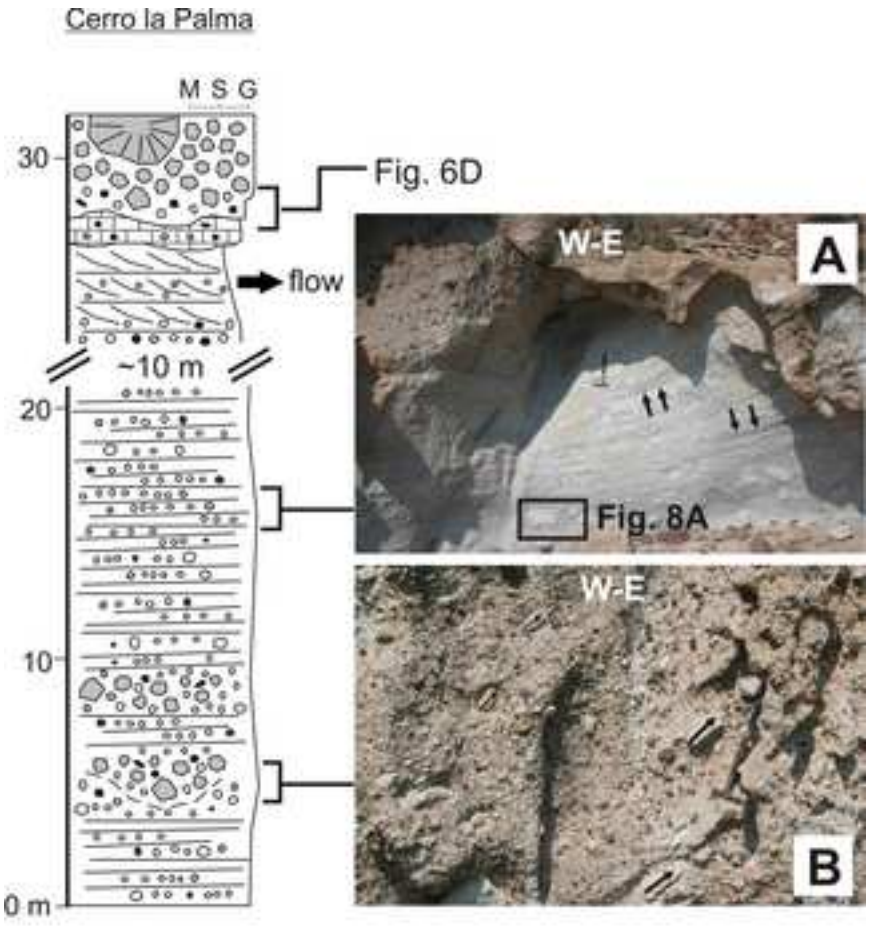

Fig. 7

Figure
Click here to download high resolution image

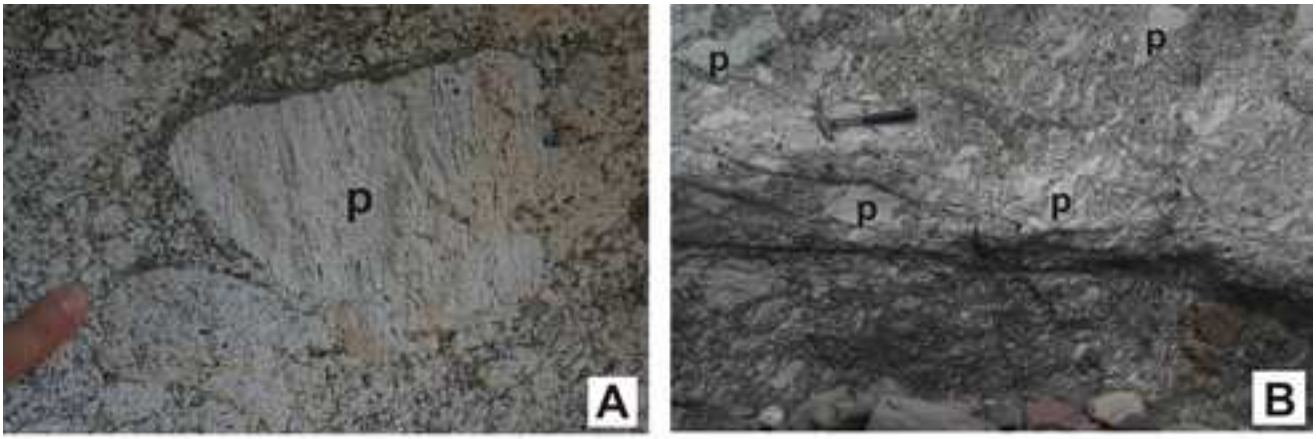

Fig. 8

Figure

Click here to download high resolution image

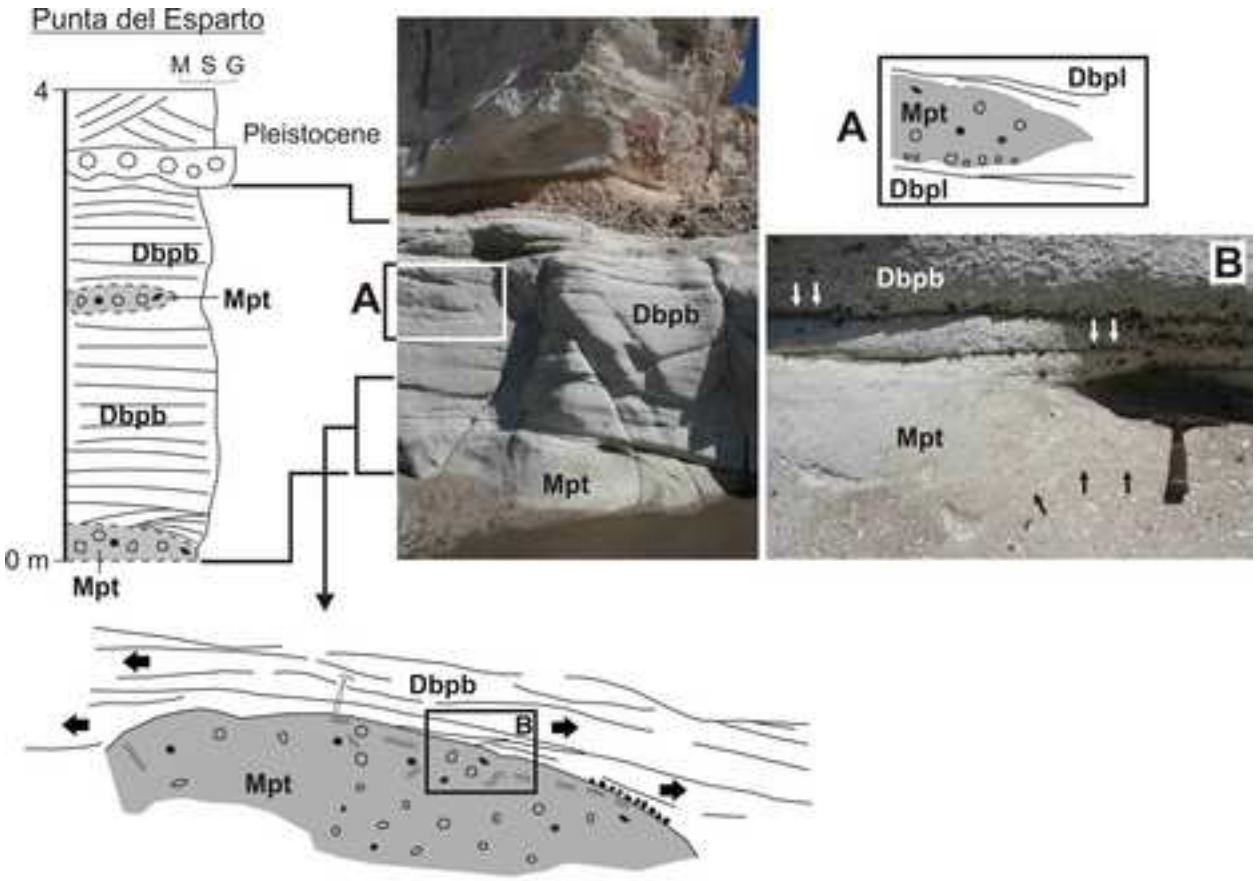

Fig. 9

Figure
Click here to download high resolution image

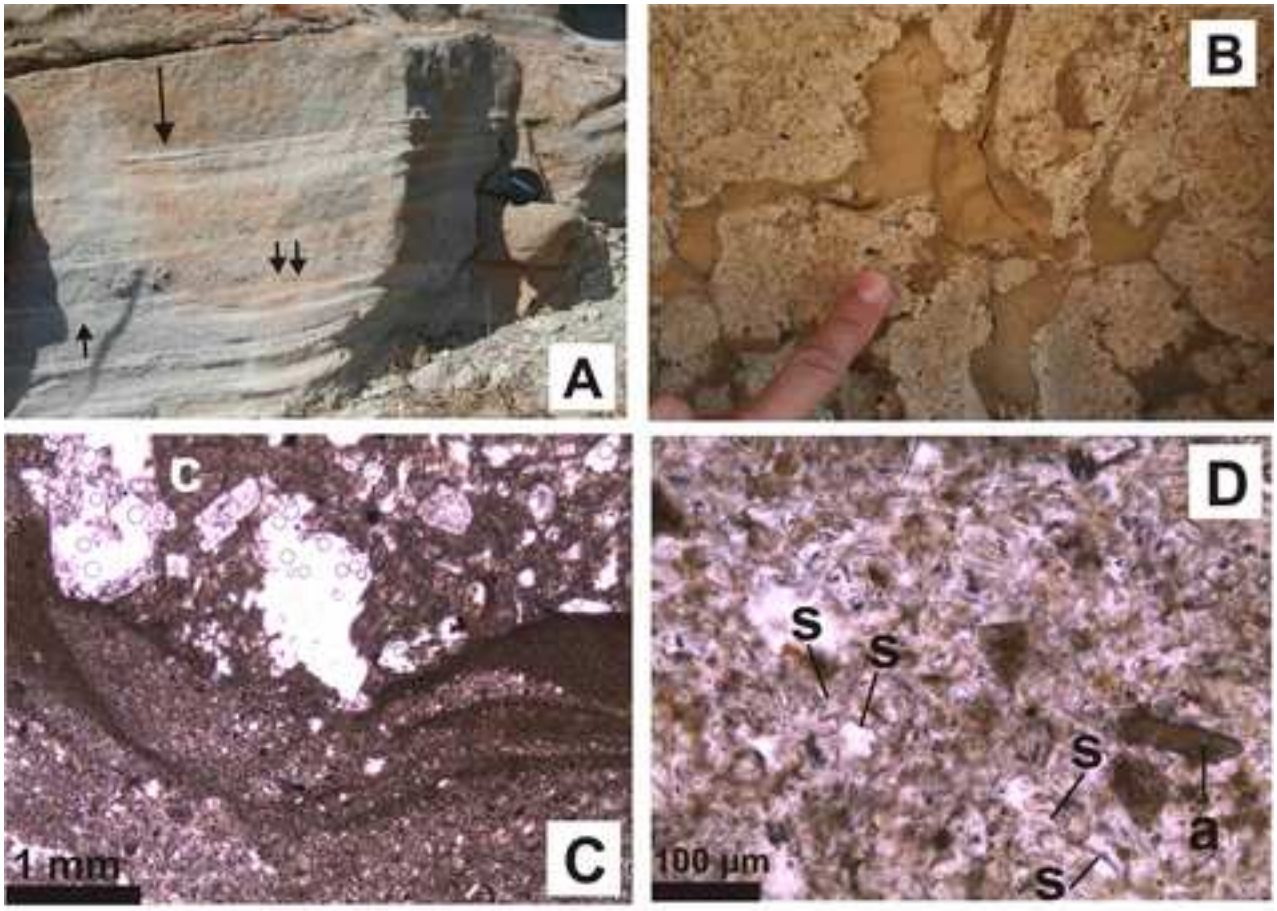

Fig. 10

Figure

Click here to download high resolution image

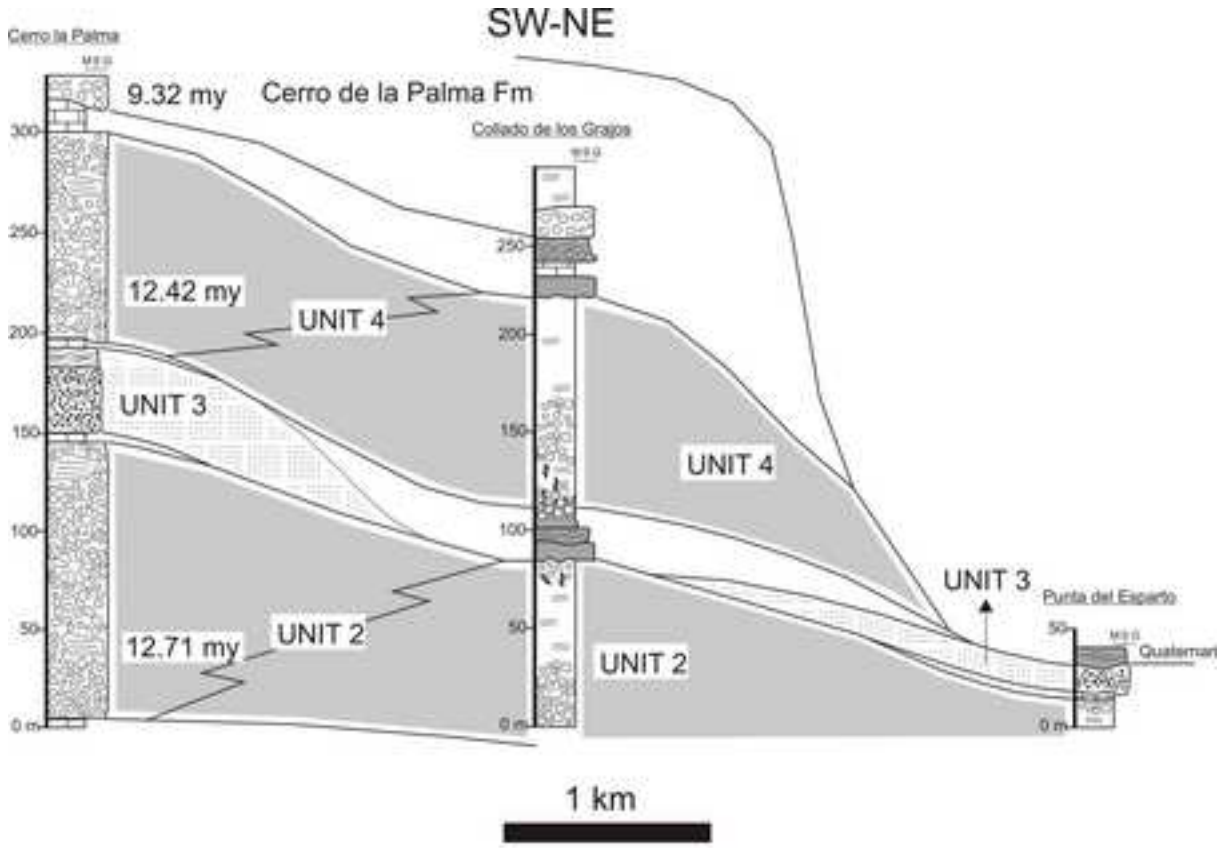

Fig. 11

Figure

Click here to download Figure: Supplementary file #1.xls

Supplementary file #1: Major and trace elements of selected volcanic rocks in Los Frailes area.

Locality	*Punta de los Frailes*	*Cerro la Palma*	*Cerro de la Palma*	*Cerro de la Palma*	*Cerro de la Palma*	*Casa del Tomate*
Latitude	36°46'14.00"N	36°46'28.00"N	36°46'11.40"N	36°46'18.00"N	36°46'25.02"N	36°46'29.00"N
Longitude	2° 4'24.00"O	2° 5'24.00"O	2° 5'39.48"O	2° 5'30.00"O	2° 5'26.40"O	2° 4'24.00"O
Sample	**ALM 71**	**ALM 49**	**CG 309**	**ALM-48**	**CG 308**	**ALM 70**
Type of sample	*breccia clast*	*coherent megablock*	*coherent megablock*	*white pumice clast*	*coherent megablock*	*coherent lava*
Stratigraphic Unit	Los Frailes Fm Unit 2	Los Frailes Fm Unit 2	Los Frailes Fm Unit 2	Los Frailes Fm Unit 3	Los Frailes Fm Unit 4	Dyke
Age (Ma)	12.71	12.71	12.71		12.42	
SiO2 (%)	62.6	63.7	63.2	66.2	64.4	63.4
TiO2	0.54	0.48	0.49	0.44	0.45	0.58
Al2O3	15.1	14.4	14.7	13.8	13.8	14.9
Fe2O3	5.30	1.77	2.71	0.77	2.55	5.30
FeO	nd	2.63	2.18	2.85	2.33	nd
MnO	0.09	0.06	0.06	0.07	0.08	0.24
MgO	3.19	3.05	3.30	1.96	3.35	2.63
CaO	5.52	5.35	5.72	4.60	5.68	6.90
Na2O	2.71	3.02	2.61	3.09	2.98	2.30
K2O	1.83	1.70	1.32	2.19	1.91	1.52
P2O5	0.18	0.11	0.10	0.13	0.09	0.21
LOI	2.91	3.67	3.63	3.89	2.37	1.95
Sum	99.96	100.00	100.00	99.97	99.96	99.92
Mg#	58.35	60.24	59.94	53.70	60.33	53.63
Sc (ppm)	22	13	15	11	15	21
V	163	154	nd	81	nd	113
Cr	11	<1	<1	< 20	7	<1
Ni	12	9	< 3	13	< 3	6
Rb	128	77	69	163	141	67
Sr	309	257	271	244	289	340
Y	17	16	9	11.9	8	24
Zr	102	126	115	135	123	85
Nb	4	7	7	7.9	5	2
Ba	309	265	275	281	282	386
La	17	nd	21	22.4	14	6
Ce	47	41	43	41.7	38	43

Major (Si, Ti, Fe^{3+}, Mn, Ca, K, and P) and trace elements have been determined by XRF at the Dipartimen
on Ignition) have been determined at the CNR-IGG of Florence. For detaile desciption of analytical methoc
Leged: nd = not determined; Mg# = [MgO]/([MgO]+0.85[FeO_{tot}])

Figure
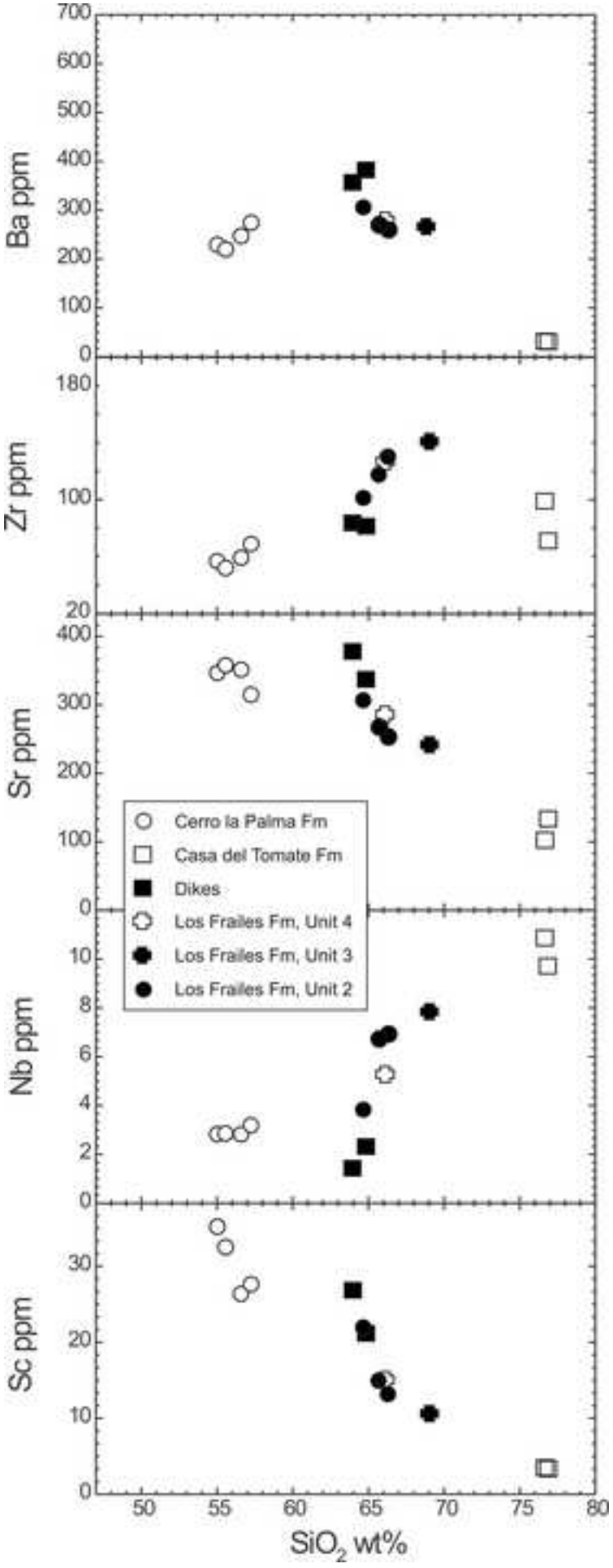
Click here to download high resolution image